NAVAL POSTGRADUATE SCHOOL
MONTEREY, CALIFORNIA

THESIS

UNMANNED AERIAL VEHICLES:
A STUDY OF
GAS TURBINE APPLICATION

by

David P. Lobik

September, 1995

Thesis Advisor: Raymond P. Shreeve

Approved for public release; distribution is unlimited.

REPORT DOCUMENTATION PAGE

Form Approved OMB No. 0704-0188

1. AGENCY USE ONLY *(Leave blank)*	2. REPORT DATE **September 1995**	3. REPORT TYPE AND DATES COVERED **Master's Thesis**

4. TITLE AND SUBTITLE UNMANNED AERIAL VEHICLES: A STUDY OF GAS TURBINE APPLICATION

5. FUNDING NUMBERS

6. AUTHOR(S)

Lobik, David P.

7. PERFORMING ORGANIZATION NAME(S) AND ADDRESS(ES)

Naval Postgraduate School
Monterey CA 93943-5000

8. PERFORMING ORGANIZATION REPORT NUMBER

9. SPONSORING/MONITORING AGENCY NAME(S) AND ADDRESS(ES)

10. SPONSORING/MONITORING AGENCY REPORT NUMBER

11. SUPPLEMENTARY NOTES The views expressed in this thesis are those of the author and do not reflect the official policy or position of the Department of Defense or the U.S. Government.

12a. DISTRIBUTION/AVAILABILITY STATEMENT
Approved for public release; distribution is unlimited.

12b. DISTRIBUTION CODE

13. ABSTRACT *(maximum 200 words)*

A survey of commercially-available gas turbine, spark and compression ignition engines was conducted to evaluate their current and future relative suitability for the DOD's unmanned aerial vehicle (UAV) short and close range program. The effects on performance associated with reducing gas turbine engine size from full scale to UAV dimensions were examined. A small turbo-jet engine (produced in France for remotely piloted vehicles) was procured in order to evaluate what levels of performance, power and endurance potential are currently achieved in commercially-available small engines. An engine test rig was designed and built to conduct performance tests. The engine was installed, instrumented and operated successfully through a series of five to eight minute tests. Selected measurements form the test stand were entered into an engine performance code in order to establish what component efficiencies and cycle parameters were required for the code to output the measured values of specific thrust and specific fuel consumption. With realistic component efficiencies thus determined, they could be used to compare gas turbine engine performance with that of other small-scale propulsion systems.

14. SUBJECT TERMS Microturbine Performance, Test rig Apparatus, Gasturb, Code Performance, JPX 240, Turbo-jet, Turbo-prop

15. NUMBER OF PAGES 89

16. PRICE CODE

17. SECURITY CLASSIFICATION OF REPORT	18. SECURITY CLASSIFICATION OF THIS PAGE	19. SECURITY CLASSIFICATION OF ABSTRACT	20. LIMITATION OF ABSTRACT
Unclassified	Unclassified	Unclassified	UL

NSN 7540-01-280-5500

Standard Form 298 (Rev. 2-89)
Prescribed by ANSI Std. 239-18 298-102

Approved for public release; distribution is unlimited.

UNMANNED AERIAL VEHICLES: A STUDY OF GAS TURBINE APPLICATION

David P. Lobik
Major, United States Marine Corps
B.S.C.E., Norwich University, 1984

Submitted in partial fulfillment
of the requirements for the degree of

MASTER OF SCIENCE IN AERONAUTICAL ENGINEERING

from the

NAVAL POSTGRADUATE SCHOOL
September, 1995

Author: David P. Lobik
David P. Lobik

Approved by: Raymond P. Shreeve
Raymond P. Shreeve, Thesis Advisor

Garth V. Hobson
Garth V. Hobson, Second Reader

Daniel J. Collins
Daniel J. Collins, Chairman, Department of Aeronautical Engineering

ABSTRACT

A survey of commercially-available gas turbine, spark and compression ignition engines was conducted to evaluate their current and future relative suitability for the Department of Defense unmanned aerial vehicle short and close range program. The effects on performance associated with reducing gas turbine engine size from full scale to unmanned aerial vehicle dimensions were examined. A small turbo-jet engine (produced in France for remotely piloted vehicles) was procured in order to evaluate what levels of performance, power and endurance potential are currently achieved in commercially-available small engines. An engine test rig was designed and built to conduct performance tests. The engine was installed, instrumented and operated successfully through a series of five to eight minute tests. Selected measurements from the test stand were entered into an engine performance code in order to establish what component efficiencies and cycle parameters were required for the code to output the measured values of specific thrust and specific fuel consumption. With realistic component efficiencies thus determined, they could be used to compare gas turbine engine performance with that of other small-scale propulsion systems.

TABLE OF CONTENTS

LIST OF FIGURES

LIST OF TABLES

I. INTRODUCTION

The Unmanned Aerial Vehicle (UAV) is a proven military concept, as was shown as recently as in the 1991 Gulf War; however, it's full potential has yet to be explored. The Department of Defense (DoD) has been, and currently is investing in the concept and charges specific agencies with the responsibility for advancing technology in this area. Currently, the UAV Joint Projects Office (UAV JPO) coordinates with the Defense Airborne Reconnaissance Office (DARO) for funding oversight of all non-lethal UAV projects. [Ref. 1] The Advanced Research Projects Agency (ARPA) of the DoD is also involved in the funding process of research projects for UAV's. The present study was funded partially by the UAV Joint Projects Office. The purpose was to examine the potential application of gas turbine engines to UAV's. The study was stimulated by recent commercial developments in very small gas turbine engines.

Until recently, the area of UAV propulsion has been left relatively unexplored compared to the larger scale propulsion systems currently used in manned flight vehicles. As avionics and control system technologies continue to advance, the propulsion area will have to advance also to extend the overall UAV system capabilities. Currently in the operational commands of the services, the propulsion needs of the close and short range UAV missions have been met with reciprocating engines. Two reasons for this engine selection is its relatively low fuel consumption and high value of power-to-weight. These two specifications are critical for the currently predominant UAV mission which is to provide real-time reconnaissance, surveillance and target acquisition support.

Several propulsion systems of various types are currently under development as part of innovative research programs. These involve a wide spectrum of initiatives including Diesel engines and gas-turbine variants. The DoD has recently shown interest

in moving away from gasoline engines to standardize on heavier, safer fuels such as kerosene, Heavy fuel is now a requirement for most exploratory development projects [Ref. 2]. Because of the aerodynamic and machine design problems inherent in scaling down gas turbines and the poor performance associated with small-scale, their use in UAV's initially appeared to be less than promising. However; extremely small (less than 20 lbs thrust) turbojet engines have recently been marketed successfully, and a new assessment needs to be made.

Over 40 years ago, turbojets and turboprops began to replace reciprocating engines in commercial and military aircraft because of their performance, reliability and maintainability. This evolutionary process may be occurring again in UAV propulsion. The turbojet is not able to compete with piston-driven engines when it comes to fuel efficiency. As was done in the past in larger engines, incorporating a power turbine into the small turbojet leads to the possibility of small turboprops approaching piston-engine fuel economy but with much better reliability and serviceability. [Ref. 1]

In the present study, first a limited survey was conducted to determine the state of the art in UAV propulsion. Performance specifications on specific engines were collected to determine trends in size, weight, power and fuel efficiency. A JPX-240 microturbine was procured in order to determine first hand what design parameters the manufacturer was able to achieve with a propulsion system of this size. The JPX-240 engine, which was developed and produced in France, was the only microturbine commercially available in its size. An engine test rig was designed and built to conduct a static performance evaluation of the JPX-240. The engine was operated successfully over a period of several weeks. Data were collected once the test apparatus was fully instrumented and operationally verified.

Concurrently, a review of available engine performance codes was conducted to determine which would most accurately model the engine test conditions. Program *GASTURB* was found to reproduce the measured engine performance well when conditions for the test were input and specific selections of component efficiencies were

made. It was concluded that the code, with component efficiencies now known to be realistic, could be used to project the potential performance of small turboprop engines for UAV applications.

II. POTENTIAL UAV PROPULSION SYSTEMS

To meet the UAV mission needs, propulsion research and development (R&D) efforts are focused on keeping the engine size and fuel consumption rate down while maintaining a high power-to-weight ratio. This goal has been the motivation of large engine manufacturers for many years. Maintenance, reliability and cost are also important considerations for engine designers and these factors must also be taken into consideration when scaling down.

Four different engine types were examined; namely, spark ignition, compression ignition, rotary and gas turbine. Propulsion systems that currently power manned-flight vehicles were examined as a start for the survey. Information on various types of engines that are currently in use for manned and umanned air vehicles were obtained from various publications and engine manufacturers. Drone engines and Auxiliary Power Units were also considered to be potential systems for UAV's. The majority of the data on engine types was found to be in the reciprocating and gas turbine categories. Rotary and diesel engines were available commercially for flight vehicles but the data available were few. Moreover, their reliability, maintenance and power-to-weight ratios have not competed well in the past with other types.

A. PERFORMANCE OF DIFFERENT ENGINES

The specific fuel consumption and associated range capability of reciprocating and turbojet engines are compared in Figures 1 and 2 respecively. While the comparison is shown for high performance aircraft, the principles are the same for all flight vehicles. Reciprocating engines realize their best propulsive efficiency at much lower flight speeds, thus obtaining better fuel consumption than the turbojet. Not until the turbojet flies at the higher flight speeds can it match and exceed the reciprocating

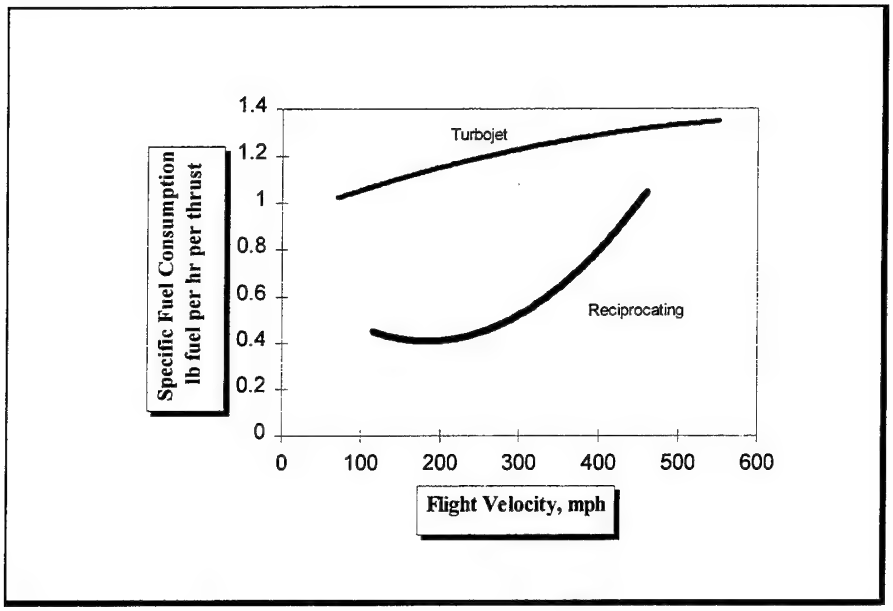

Figure 1 Specific Fuel Consumption Comparison After Ref [3]

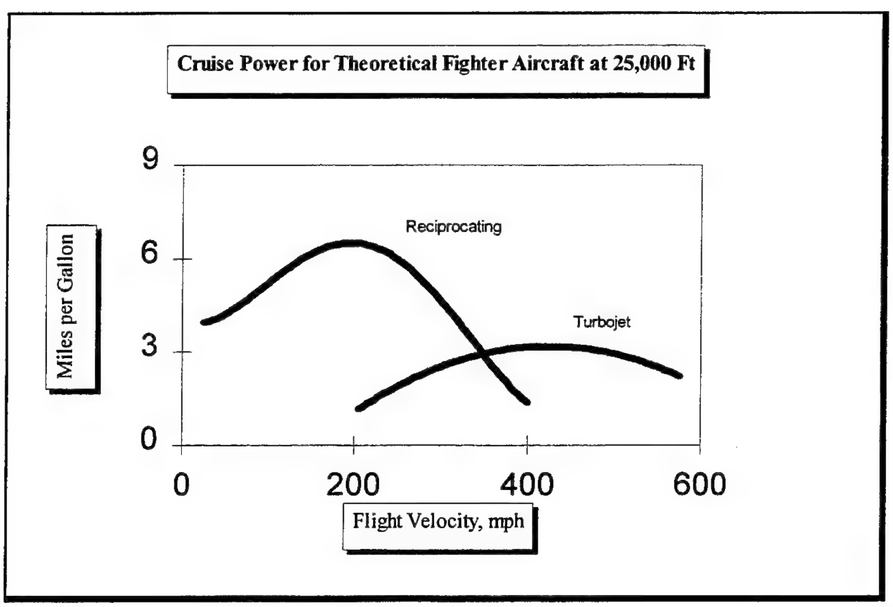

Figure 2 Specific Range Comparison After Ref [3]

engine in specific range. This is due to its improved propulsive efficiency at higher flight speeds.

The thrust power available from reciprocating and turboprop engines at increasing airspeeds are compared in Figures 3 and 4. These figures show some of the advantages turboprops have over reciprocating engines. As can be seen, the turboprop performance exceeds that of comparable reciprocating engines from the lowest speeds. Not only is thrust produced by the engine exhaust nozzles, there is much less drag associated with the air intake and engine cross-sectional profile.

An extensive search for performance information on small gas turbine engines (microturbines) for flight vehicles was conducted. Janes' [Ref. 4] and AW&ST [Ref. 5] provided little information on engines in the 700 lb thrust class and below, subsequently, manufacturers were consulted directly. Most of the larger aircraft engine manufacturers in the U. S. and Europe had not viewed these smaller engines as profitable in the past; consequently, little R & D went into them. Most gas turbine engines in this class were developed for target drones and remote-control model enthusiasts. Data for the specific fuel consumption (SFC) of small turbojet engines in this low thrust category are shown in Figure 5. A trend evident in the figure is the increase in SFC with decrease in engine thrust. There are many reasons for this, but most importantly, the aerodynamics of the very small components in these engines are inevitably accompanied by sizable losses.

Providing a reference for direct comparison in performance between turboprop and reciprocating engines is difficult. Most manufacturers of reciprocating engines publish a brake-mean-effective pressure (bmep) as a measure of performance of the cycle itself. Brake specific fuel consumption (BSFC)'s are sometimes given, but again, it is not conventionally used as a primary performance measurement. However, a turboprop's performance is measured in (BSFC). A comprehensive survey of engine manufacturers was conducted by Dev [Ref. 6]. He found the reciprocating engines in the horsepower range of approximately 400 and below achieved BSFC's in the range

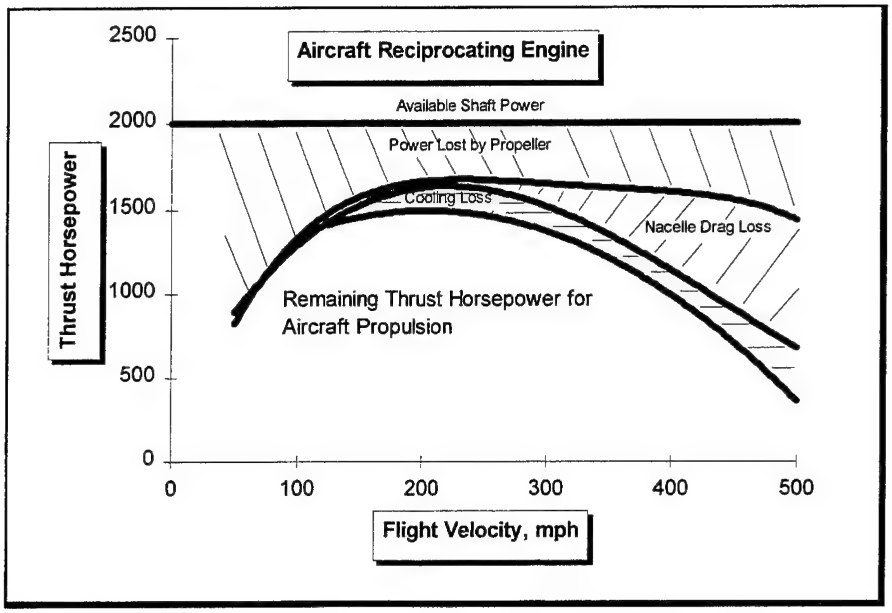

Figure 3 Performance Comparison, Reciprocating Engine After Ref [3]

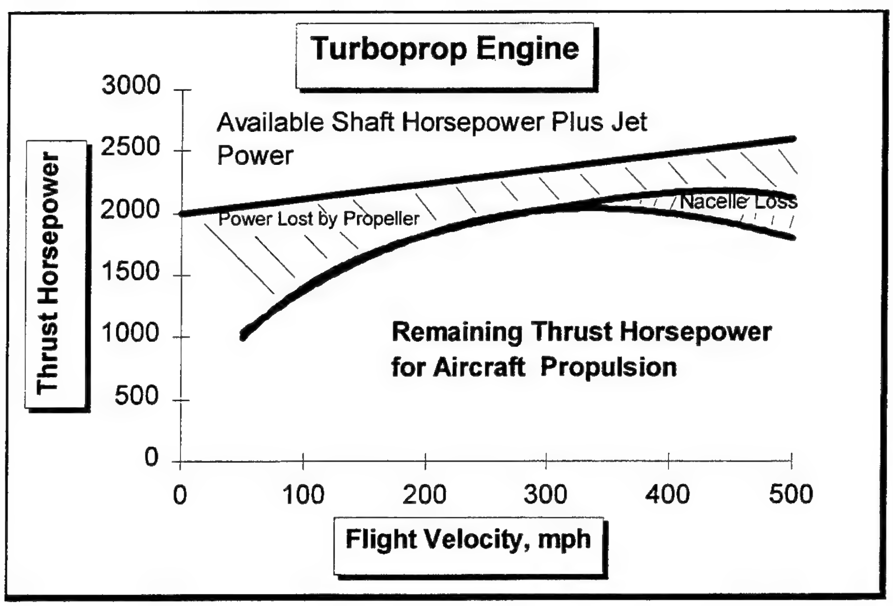

Figure 4 Performance Comparison, Turbo-prop After Ref [3]

of 0.5 to 1.0 lb/hp/hr. As indicated by aircraft engine company, M-DOT Inc. [Ref 2: p. 48], manufacturers of small turboprops believe that they must achieve BSFC in the range of 0.5 to 0.6 lb/hp/hr before these engines will be acceptable.

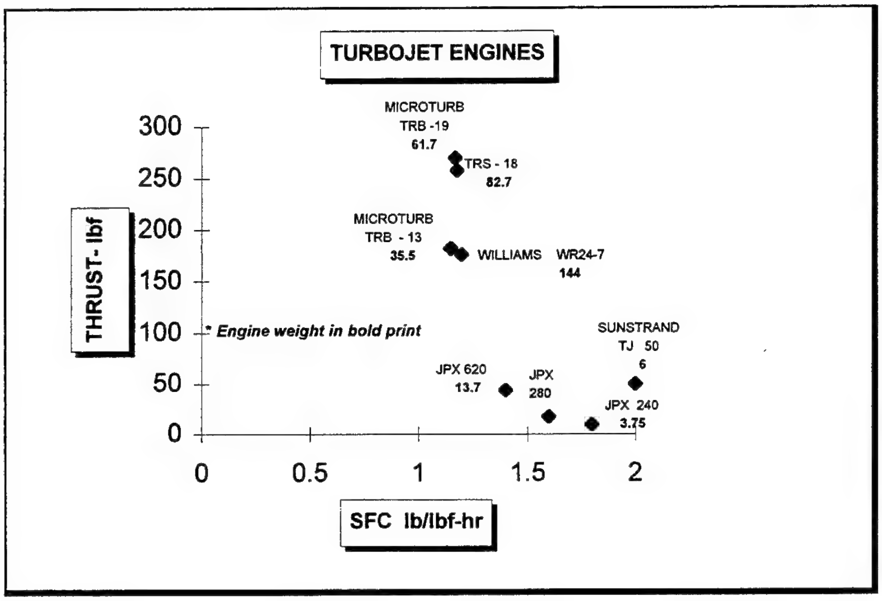

Figure 5 Turbojet Summary

Data for small turbo-shaft engines are given in Figure 6. The observable trend here is that the turbo-shaft engines are heading toward the BSFC's of the reciprocating engine for roughly the same horsepower. An additional problem presents itself with small turbo-prop engines. The small reduction gear-box must handle the tasks of reducing a very high engine RPM to the relatively low RPM for a propeller, still be light weight and have a reasonable fatigue life. All are significant challenges.

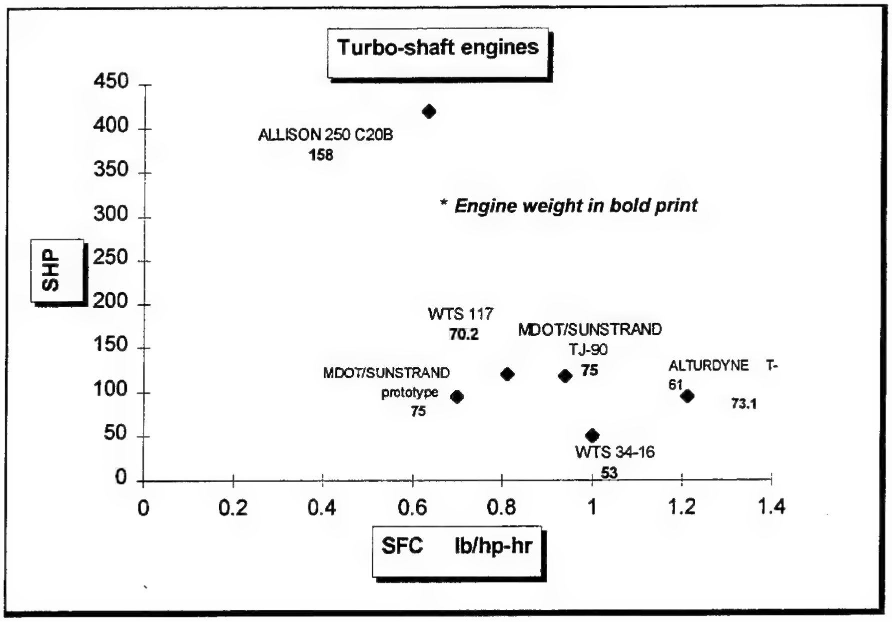

Figure 6 Turboprop Summary

B. CONSIDERATIONS IN SCALING DOWN

1. Reciprocating, Spark Ignition Engines

Both two-stroke and four-stroke engines have been considered. Four-stroke engines are typically more fuel efficient than two-stroke engines. The additional strokes in the cycle allow engines greater charge retention and purity, and thus higher thermal efficiency. The disadvantage of four-stroke engines when compared to two-stroke engines is the lower power-to-weight ratios. The two-stroke cycle theoretically provides twice the power per cycle that the four-stroke cycle provides, for an engine of the same size and revolutions per minute (RPM). This potential is not realized in practice due to the poorer scavenging in the two-stroke cycle, which can result in losses of up to 40 %. [Ref. 3 & 7] Increasing RPM is a way of increasing power in both cycles. However, increasing the rate of power strokes tends to cause excessive heating of the engine parts and can cause breakdown of the lubrication and therefore reduced life. When scaling-down engines, the scavenging process becomes disproportionately

less efficient, and power drops off as well. However, the advantages of the two-stroke engine outweigh the disadvantages; thus it has been preferred to date in UAV's.

There are many more factors that affect reciprocating-engine performance such as carburation, fuel injection, timing and exhaust blowback, but the smaller the scale of the engine, the more difficult it becomes to improve its efficiency and performance. Cycle augmentation methods have been pursued such as turbocharging and incorporating heat exchangers, but there is always a compromise with weight. One promising development area for these engine types is ceramics. The greater heat retention, higher strength and lower weight of ceramics is likely to play a major role in the future.

2. Diesel Engines

Difficulty is experienced in scaling down Diesel engines to reasonable weights for use in UAV's. Most compression-ignition engines rely on compressing the air until the end of the compression stroke is reached, at which time fuel is injected into the cylinder. Due to the very high temperatures reached after compression, the fuel-air mixture automatically ignites. Very high peak pressures usually occur in this process so that heavy, high strength cylinder heads are required, resulting in low power-to-weight ratios.

There are additional drawbacks that must be overcome before diesels are acceptable for the UAV. Problems in exhaust emissions occur in diesel engines when the fuel-air mixture barely surpasses the chemically correct ratio. "Black smoke" is easily produced which is undesirable in tactical air vehicles. Other factors affecting the performance of the compression ignition engine include injection timing, timing of valves and ports, blow-down and pumping losses. [Ref. 3 &7]

3. Rotary Engines

Rotary engines have been used in manned flight vehicles in the past, but not to any large extent. The main reason has been lower reliability and lower power-to-weight ratios. These engines have not competed well with reciprocating and gas turbine engines for these reasons. Teledyne Continental's GR-18 Wankel engine for UAV's is one of the few that are available. The engine produces 45 hp at 7500 RPM (50lbs dry weight). It's power-to-weight ratio is less than unity, whereas reciprocating and gas turbine engines typically exceed unity. [Ref. 8]

4. Gas Turbine Engines

Very small gas turbine engines were not available commercially until very recently. Today, various models are available to the remote-control aircraft modeler. With advances in technology, microturbines are becoming commercially competitive as evidenced by advertising in the remote-control modeling literature and, more noticeably, in the number of engine manufacturers competing for DARO contracts. The major reason for the delay in microturbines arriving in commercial markets was the difficulty in achieving acceptable performance when scaling down to drone or UAV size. Reasons for poorer performance in smaller scales include the following;

- Reynolds Number Effects. The aerodynamic performance of blading suffers greatly when scaling down. At the lower Reynolds numbers associated with small scale, higher coefficients of friction occur, which result in lower component efficiencies.

- Larger Relative Tip Clearances. In turbomachinery systems, the minimum operating tip clearance is almost an absolute amount. The ratio of tip clearance to the span of the blade is then much greater in smaller than in full-scale engines, resulting in proportionately greater losses.

- Lower Cycle Pressure Ratios. Centrifugal compressors are favored in smaller gas turbines because of the higher pressure ratios that can be achieved in single rotor. The drawback is that the centrifugal compressor

efficiency is relatively low above ratios of 6 or 7 due largely to friction and tip clearance losses. To achieve the higher pressure ratios that are needed, a combination of centrifugals, axial and centrifugal, or purely axial compressors is required. In axial compressors, the blade passage area decreases from the front of the compressor to the rear, and blades must be reduced in height. When reducing the compressor size, these blades become extremely small. Because high cycle pressure ratios lead to vanishing by small blade heights, lower pressure ratios are inevitable. [Ref. 6 & 9]

- Lower Peak Cycle Temperatures. In larger engines, the turbine blades are cooled using various methods. A common technique is to pump bleed air through passages inside the blades. Microturbines cannot accommodate this type of cooling because their small size. For this reason small engines are limited to lower peak cycle temperatures. [Ref. 6 & 9]

- Difficulty of Manufacturing. Because microturbine blading is so small, tighter tolerances are required during manufacture to achieve the same precision in aerodynamic shaping . This results in higher costs.

An increase in the thermal efficiency of the gas turbine cycle means a decrease in the specific fuel consumption. Engines that are based on the recuperated gas turbine cycle can have much lower SFC than the basic gas turbine engine. Recuperation involves passing high temperature turbine exit air through a heat exchanger in order to recover the energy by raising the temperature of the air leaving the compressor. Heat-exchanger efficiencies are typically in the 0.7 to 0.8 range. It has been shown by cycle analysis that cycle pressure ratios for the recuperated engine should be much lower than those required for the non-recuperated engine. Application of recuperation in flight engines requires the development of light and effective heat exchangers. Recuperation in very small gas turbines would relieve the requirement of achieving very high pressure ratios with very small components.

III. PERFORMANCE CODES

To model the JPX-240 performance cycle, four programs available at the Naval Postgraduate School for engine-cycle analysis were reviewed for capability and accuracy. The results of this review are discussed below, followed by a comparison between the four codes using the same design limitations as inputs.

A. THERMOWARE

Thermoware was written at Stanford University by Professor R.H. Eustis.

1. Assumptions

- Working fluid is treated as an "ideal gas" with constant specific heats
- Steady flow of working fluid and no transient effects
- Changes in kinetic and potential energy are negligible for compressors, expanders and heat exchangers

2. Capabilities

- Handles all gas turbine types
- Evaluates cycles with single or multiple components
- Regenerative cycle to evaluate regenerator effectiveness

3. Limitations

- No 'off-design' capability
- Does not consider cooling air, bleed air, power takeoff
- Cannot vary lower heating values
- Inlet, burner and nozzle losses are not considered
- Cannot iterate on variables
- Specific heats are constant through the cycle

4. Output flexibility

- Result of cycle output to screen only, not to data file
- Plotting routine incorporated but to screen only

B. ONX/OFFX VERSION 2.1

This engine performance code was written by Jack D. Mattingly. The code was developed for use with an aircraft engine design text. [Ref. 10]

1. Assumptions

- Flow is steady on average
- Flow is one dimensional at the entry and exit of each component
- Fluid behaves as a calorically perfect gas with constant specific heats

2. Capabilities

- Off-design can be calculated
- Can select turbojet with and without afterburner, 'turbofan', 'turboprop' and 'ramjet'
- Values of Cp, Cv, gamma and R can change across burner, mixer and afterburner
- Bleed air, cooling air and bypass ratio are inputs
- Lower heating value is an input
- Perfect gas constants are inputs
- Component figures of merit are inputs
- Iterates Mach #, maximum temperature leaving main burner, compressor ratio, fan pressure ratio and bypass ratio

3. Limitations

- No regenerative cycle analysis capability
- Specific heats are constant

4. Output flexibility

- No plotting capability
- Results can be output to the screen or to a data file

C. ENGINE

Engine was written by A. Mathur for the Naval Postgraduate School [Ref. 11]. It is a performance code that calculates the cycle for a mixed-exhaust, two-spool, cooled, afterburning turbofan engine with and without a wave-rotor component.

1. Assumptions

- Flow considered steady on average
- Fluid treated as "half-perfect gas"
- Specific heats are functions of temperature, expressed as polynomials.
- Cooling air is taken from high pressure compressor to high pressure turbine
- No cooling is provided for the low pressure turbine
- The engine is assumed to have a variable area converging/diverging nozzle with complete expansion.

2. Capabilities

- Can iterate on variables
- Variable specific heats (gives greater accuracy)
- Input component efficiencies, pressure losses across burner and mixer, lower heating value
- Enthalpy of fuel is considered

3. Limitations

- No regenerative cycle capability
- Turbojet and turbofan only

4. Output flexibility

- No plotting capability
- As it stands, cannot write data to a file

D. GASTURB

Gasturb was written at MTU in Germany as a program to calculate design and off-design performance of gas-turbines [Ref. 12]. The program models most features which are present in gas turbine engines and is careful to include the effects of varying specific heats.

1. Assumptions

- Working fluid is assumed to behave as a "half-ideal gas"
- Cp is (for air or air and combustion products alike) only a function of temperature. [This is a very good approximation to reality for the operating range of gas-turbines].

2. Capabilities

- ♦ Calculates off-design performance
- ♦ Power takeoff, cooling air, bleed air and bypass air are inputs
- ♦ Parametric studies: single point calculation, iterate on a variable, effects on a cycle, series of cycles and optimization
- ♦ Design choices - same as ONX

3. Limitations

- ♦ No regenerative cycle capability
- ♦ Lower heating value is fixed at 18,530 BTU/lbm

4. Output flexibility

- ♦ Sends data to the screen, or to a file
- ♦ Can send plots to an HP printer only
- ♦ Can save plots as HPGL file for import to word processor software

E. COMPARATIVE STUDY

To compare the predictions of the four codes, a test case of a simple turbojet was conducted with the inputs shown in Table 1. No bleed air, power take-off or cooling air were allowed, and where some programs have additional pressure ratio and efficiency inputs, they were set to unity to provide equal conditions for each program.

Flight Conditions	Design Limitations	Output
Mach # 0.0	πc 5	mf fuel flow rate
To 519 deg R	ηc 0.80	F Thrust
Po 14.7 psi	ηt 0.85	F/mo Specific Thrust
	ηb 0.98 Tt_4 1900 °R	SFC Specific Fuel Consumption
	Air Flow Rate-1.25 lbm/sec	
	LHV - 18,530 BTU/lbm	

Table 1 Input and Output Parameters in Code Comparative Study

The results obtained are shown in Table 2. The results indicate that higher SFCs were given by the programs that treat specific heats as being constants.

	Thermoware	Onx/Offx	Engine	Gasturb
mass flow - air lbm/sec ***Input**	1.25	1.25	1.25	1.25
mass flow - fuel lbm/sec	.023	.024	.014	.019
Thrust lbf	69.43	66.41	69.88	72.41
Specific Thrust lbf/lbm/sec	55.54	53.13	54.90	57.93
SFC lbf/lbm-hr	1.204	1.314	0.724	0.937

Table 2 Performance Code Output

F. REGENERATIVE CYCLE ANALYSIS

Regenerative cycles have been identified as a possible option to increase thermal efficiency, thereby reducing fuel consumption [Ref. 2]. To develop an understanding of the benefits that the regenerative cycle can provide, a series of "engines" were calculated using the engine cycle analysis program, *Thermoware*. The turbojet cycle option was used to generate a performance map. A similar performance plot was constructed using the regenerative turbojet cycle option. Efficiencies input into the program were arbitrarily chosen.

Figures 7 and 8 are plots of engine performance calculated for six compressor pressure ratios (Prat) at six different maximum combustion chamber temperatures (also referred to as Turbine Inlet Temperature (TIT)). Figure 7 shows the pure turbo-jet cycle performance. Several trends are apparent:

- The net work and thermal efficiency increase as the turbine inlet temperature (TIT) increases.
- The maximum work is not necessarily at the point of maximum thermal efficiency.
- There is an optimum Prat at a given TIT that provides the most work.
- As TIT increases, the Prat for maximum net work decreases

It was observed that the results given in Figure 7 were in reasonable agreement with those given by Boyce [Ref. 9: P. 35].

Figure 8 shows the regenerative cycle performance. The trends are similar to those of the turbojet; however, some additional trends are evident:

- The thermal efficiency is notably increased
- As TIT increases, Prat for maximum net work increases.

Again, the results in Figure 8 were in reasonable agreement with those given by Boyce [Ref. 9: P. 38]. Figure 9 shows a comparison between the two cycles at three pressure ratios. These data were extracted from Figures 7 and 8 to provide a picture of the differences between the cycles. The trends are listed below.

- As Prat increases, the thermal efficiency benefit of regeneration decreases.
- The greatest increase in thermal efficiency is at a Prat of 2.5; therefore, the greatest benefits from regeneration for a given TIT occurs at low pressure ratio.
- TIT provides the greatest thermal efficiency increase at the lowest pressure ratios.
- Thermal efficiency levels off as Prat and TIT become large .

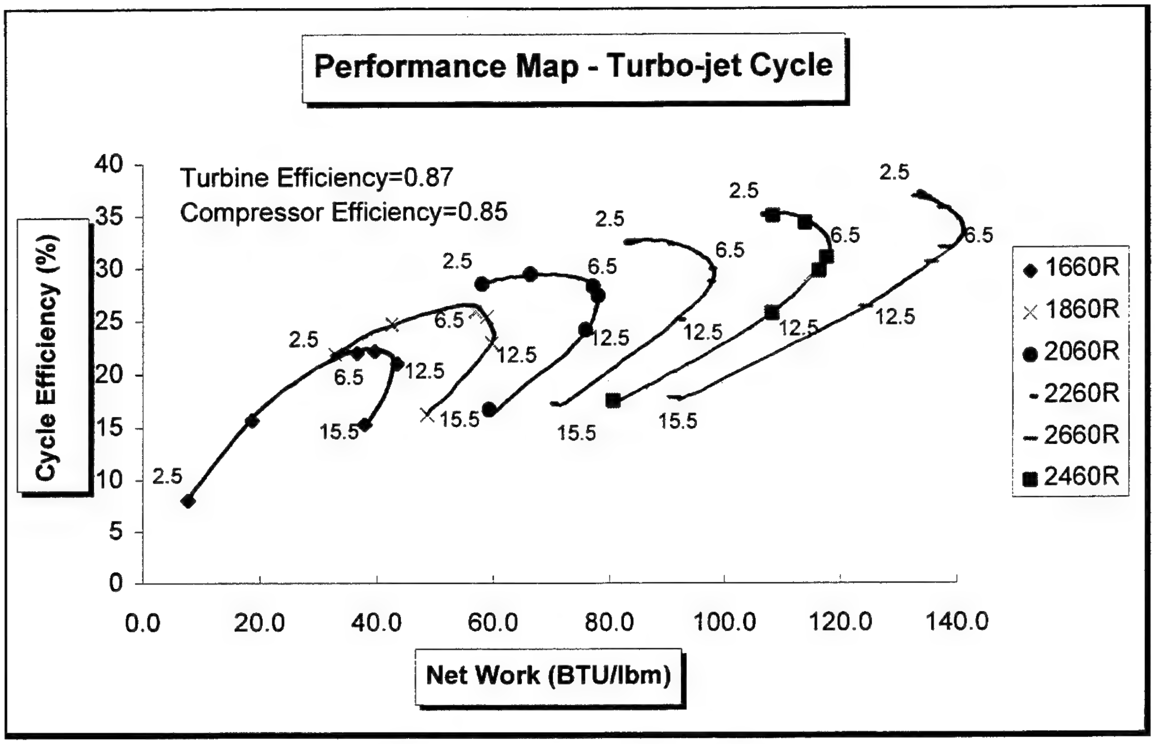

Figure 7 Turbo-jet Cycle Results

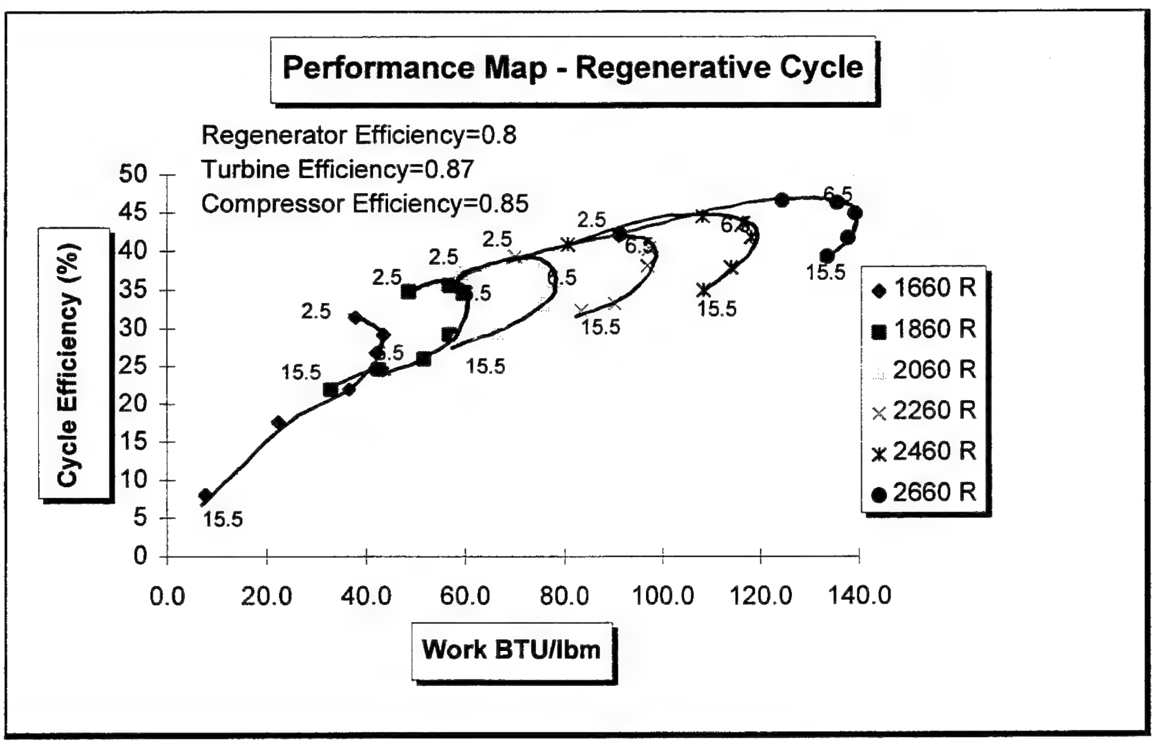

Figure 8 Regenerative Cycle Results

In summary, the regenerative cycle provides the benefit of giving better cycle efficiency at lower pressure ratios with a minimal change in net work. This is highly desirable for a small engine for a mission that requires long ranges or loiter times.

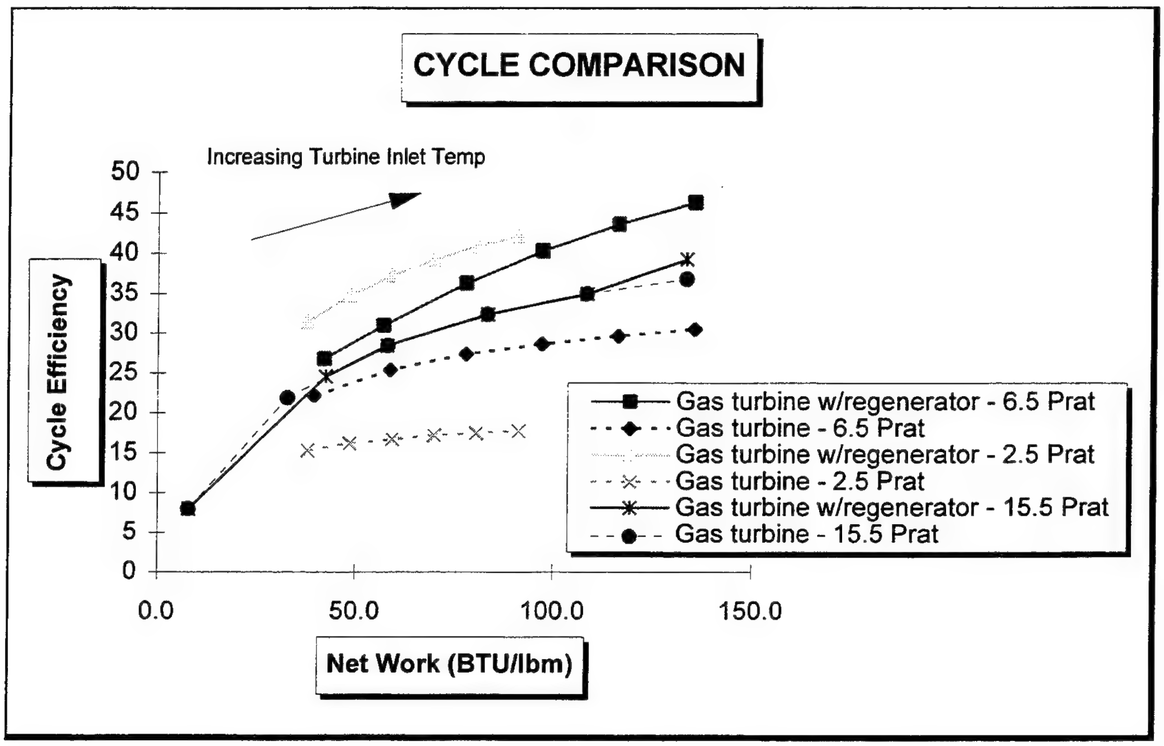

Figure 9 Recuperated Turbo-jet vs Pure Turbo-jet

IV. ENGINE TEST PROGRAM

A. JPX-240 MICROTURBINE

The JPX-240 was, at the time this research began, the smallest of a family of microturbine engines produced by JPX in France. JPX targeted the remote-control model industry as the primary customer for the engine. Although other engine manufacturers were involved in research and development to produce microturbines, the JPX-240 was the only engine that was commercially available in this range of very low thrust. The engine's specifications are shown in Table 3.

Engine size	length = 13.18 in, diameter = 4.56 in
Weight	3.75 lbs
Fuel	Liquid propane
Performance	8.83 lbf thrust @ 120,000 RPM SFC = 1.806 lb/lbf-hr
Compressor	Single stage, light alloy, centrifugal
Turbine	Special refractory alloy, single radial-inflow turbine rotor
Lubrication	Self-feeding oil lubricating system
Bearings	high-speed, high precision, ceramic-ball bearings
Ignition	Single spark and CDI ignition system
Starting System	Compressed air

Table 3 JPX-240 Specifications After Ref. [13]

B. TEST APPARATUS

An engine test apparatus was designed and installed in the Gas Dynamics Laboratory (Bldg. 216) at the Naval Postgraduate School. The apparatus is shown in Figures 10 and 11. Detailed drawings are given in Appendix A.

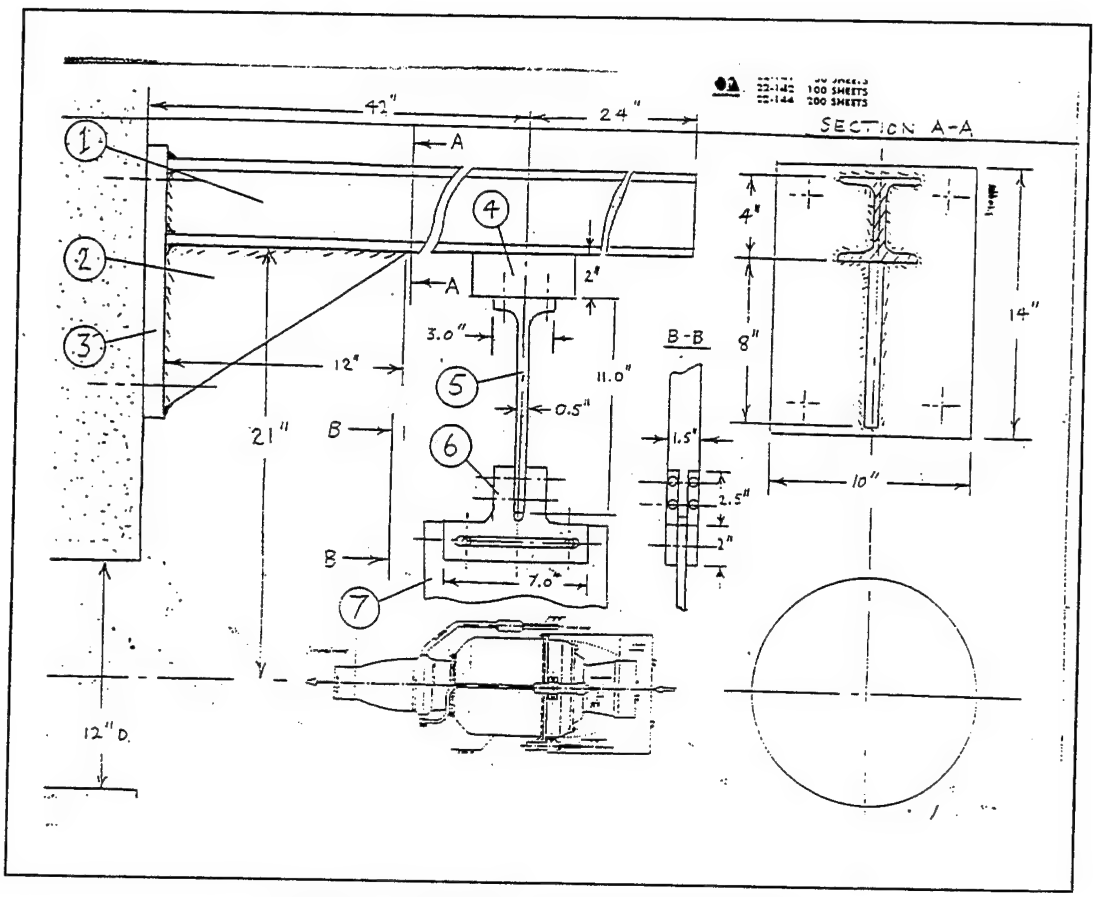

Figure 10 Engine Test Rig Schematic

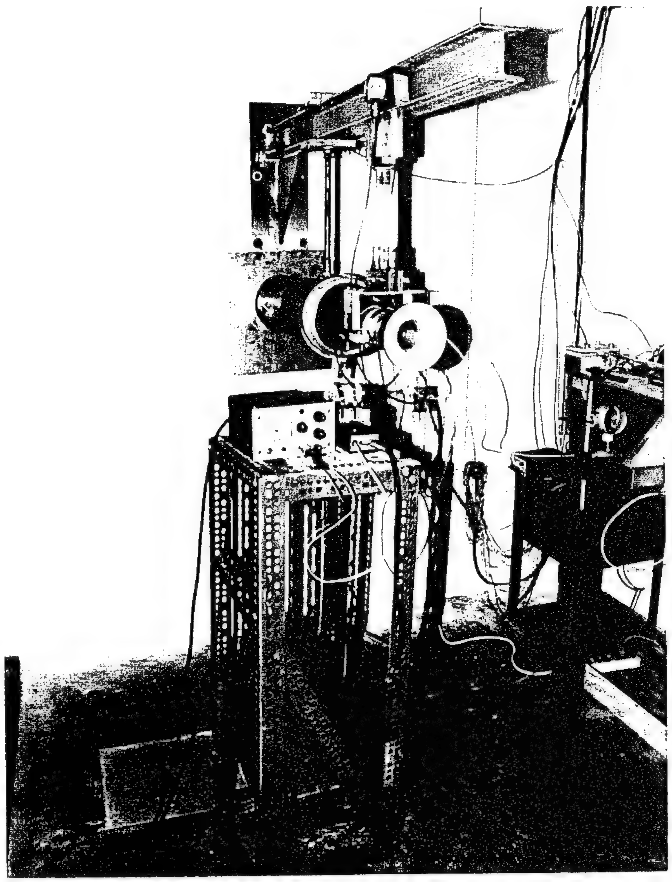

Figure 11 Engine Test Apparatus

A 66 inch x 4 inch I-beam was welded to an attachment plate which was bolted to the northeast wall in Bldg. 216. A 12 inch hole was drilled through the reinforced concrete wall to accommodate an outlet duct for the engine exhaust gas. The engine was hung from the I-beam by a spacer, thrust beam and cradle, also shown in Appendix A. A partition was placed between the data acquisition area and the test rig as a safety measure.

C. INSTRUMENTATION

1. Air Flow Rate Measurement

A bellmouth assembly was designed and implemented in accordance with A.S.M.E. Power Test Codes [Ref. 14] as shown in Figure 12. The design value of the flow coefficient was 0.995, based on the Reynolds number of the flow. Four static-pressure ports (P_{port}) spaced at 90 degrees, were drilled into the throat of the bellmouth as shown in Appendix A. These four pressures and incoming stagnation or ambient pressure (P_{amb}), were sensed and recorded using a Scanivalve Zero Operate and Calibrate (ZOC) pressure system. The incoming stagnation temperature (T_{amb}) was taken to be ambient, and the flow rate was calculated using Equation 1with the following variables defined:

$A_{bellmouth}$ = area of the bellmouth throat

Y = net expansion factor for square-edged orifices

C = coefficient of discharge

F = velocity of approach factor, $\frac{1}{\sqrt{1-\beta^4}}$, where β (d/D) is the ratio of bellmouth throat diameter to the inlet diameter. In this case, D >>d.

F_A = factor to account for thermal expansion of primary element

R = specific gas constant

$$\boxed{m = A_{bellmouth} \cdot \sqrt{\frac{2P_{amb}\left(P_{amb} - P_{port}\right)}{R \cdot T_{amb}}} \cdot Y \cdot C \cdot F \cdot F_A}$$

Equation 1 Mass Flow Rate From Ref. [14]

The values given below were used in the mass flow equation. The values take into account the material and geometry of the bellmouth and compressibility of the air.

$\beta = 0$	CF = 0.995	$F_A = 1.0$	Y = 1.0

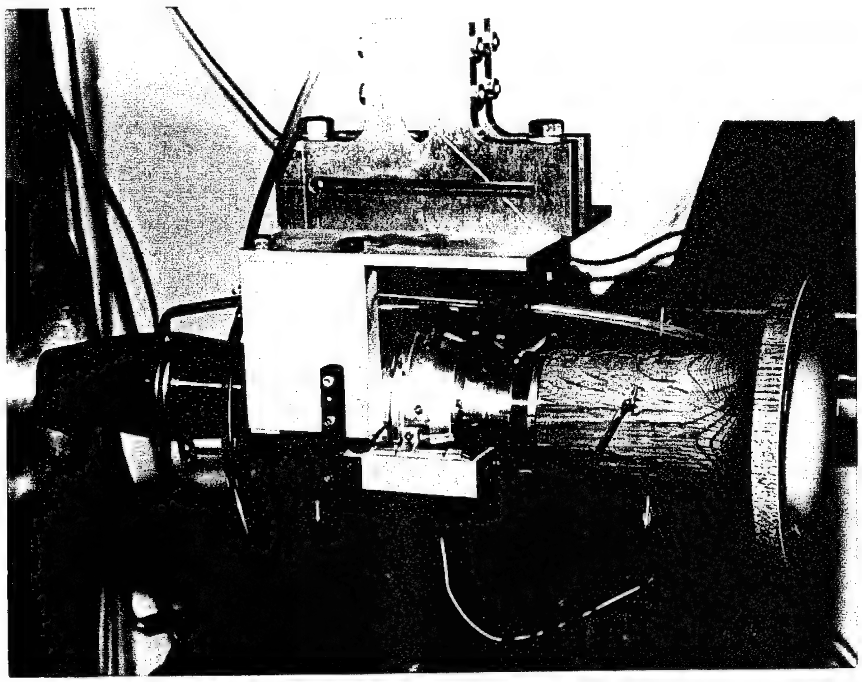

Figure 12 Bellmouth Assembly

2. Fuel Flow-Rate Measurement

To enable the on-line measurement of the fuel flow-rate to the engine, a very sensitive, low-flow meter was installed. The meter was designed for a linear range of .008 to .08 gpm. The flow meter was a jeweled-bearing, paddle-wheel type that provided a frequency signal to the data acquisition system through a charge amplifier. The meter is shown in Figure 13.

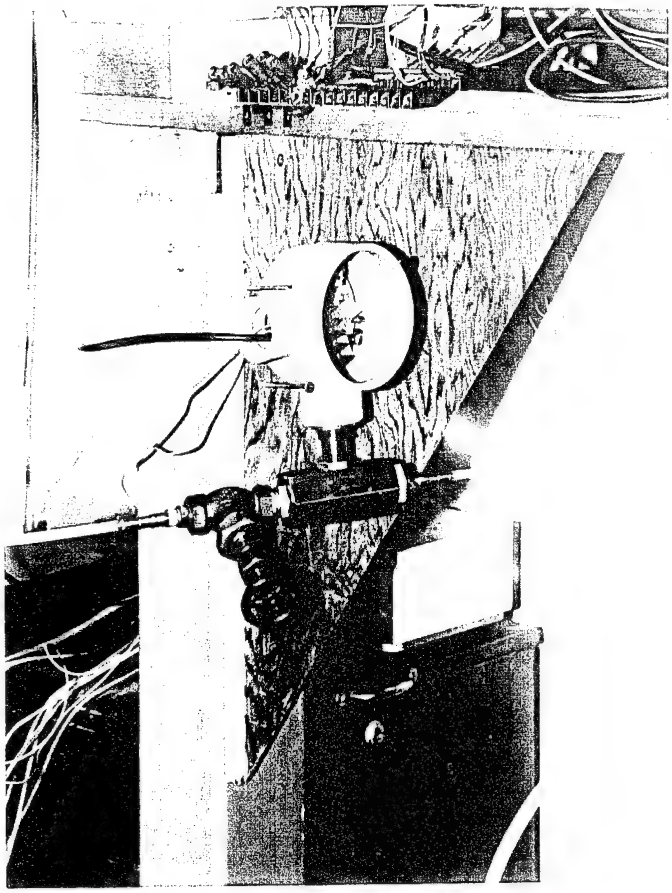

Figure 13 Fuel-Flow Meter

To provide redundancy in measurement , and to verify the calibration of the fuel-flow meter on-line, a simple strain-gage beam apparatus (with Wheatstone bridge) was installed to measure the weight of the fuel tank, as shown in Figure 14. The beam was calibrated and the results are given in Appendix B1. The data acquisition system sampled the strain-gage output voltage (thus the weight of the fuel tank), over pre-set intervals of time while the throttle was constant. This provided the most accurate and repeatable method for obtaining the fuel-flow rate.

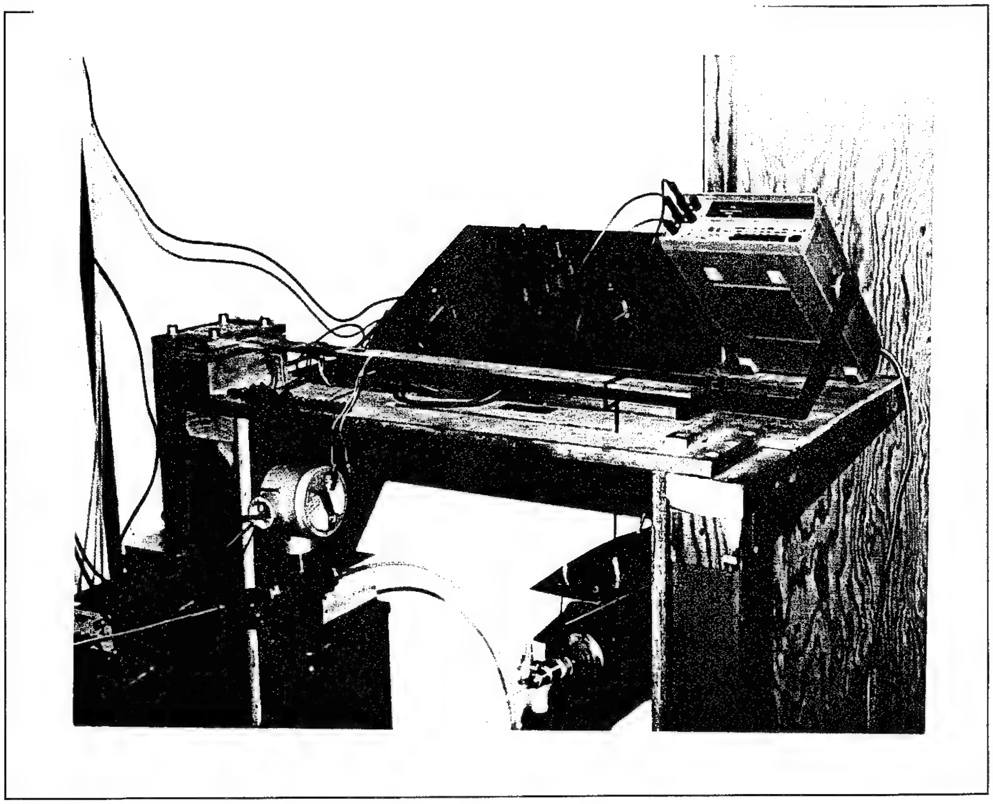

Figure 14 Fuel Flow Strain-Gage Beam

3. Thrust

The thrust was measured by the deflection in an 11-inch strain-gaged beam from which the engine was suspended. The arrangement is shown in Figure 15. Four strain gages were applied (two on each side) to provide maximum sensitivity (for accuracy) and temperature compensation. The leads were connected to a signal conditioner in the data acquisition system. The beam was calibrated by hanging weights and results are given in Appendix B2.

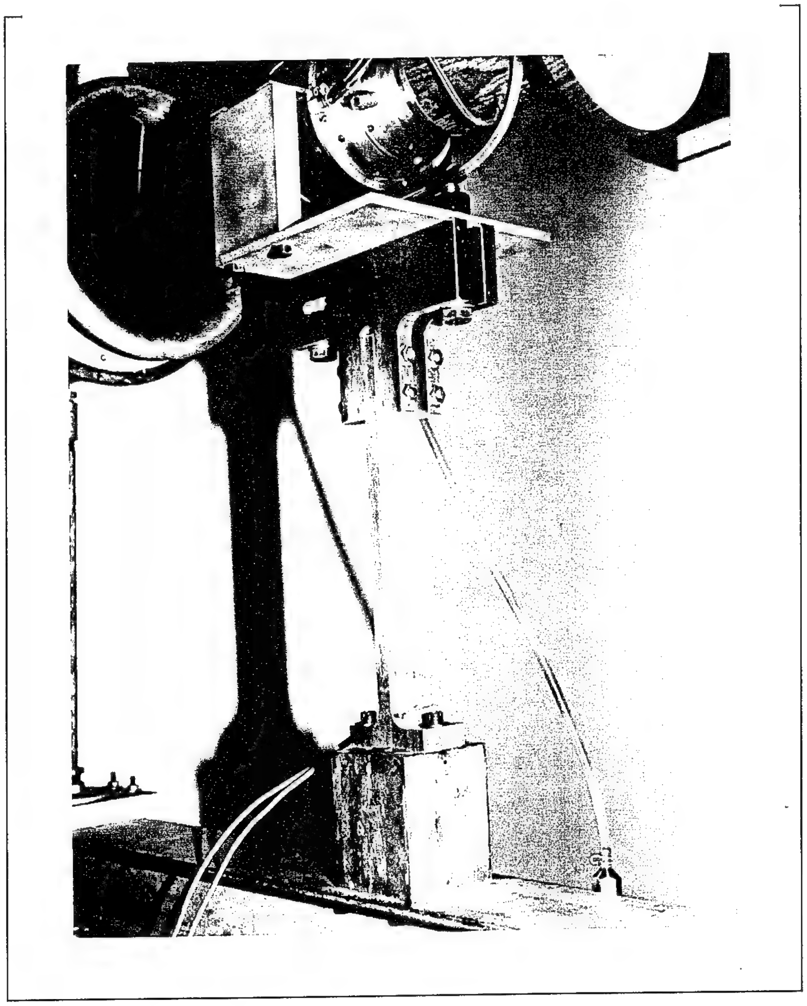

Figure 15 Thrust Beam

4. Nozzle-Exit Temperature and Pressure

The stagnation temperature and pressure were measured at the exit of the tail pipe using a commercial, United Sensor P-T probe as shown in Figure 16. The temperature measurement was not connected to the data acquisition but was recorded

manually using a digital meter. The thermocouple was a J-type, allowing accurate temperature measurement up to 760 Deg. Celsius, which was above the temperature expected in the exhaust. The exit total pressure, from the Kiel-type sensor, was recorded using the Scanivalve ZOC pressure scanning system. The probe was located 3 inches downstream of the nozzle exit plane. (The nozzle exit diameter was 1.42 inches). The pressure sensor was 0.1 inches above centerline. The temperature sensor was 0.08 inches below centerline. The probe was held fixed throughout the test program.

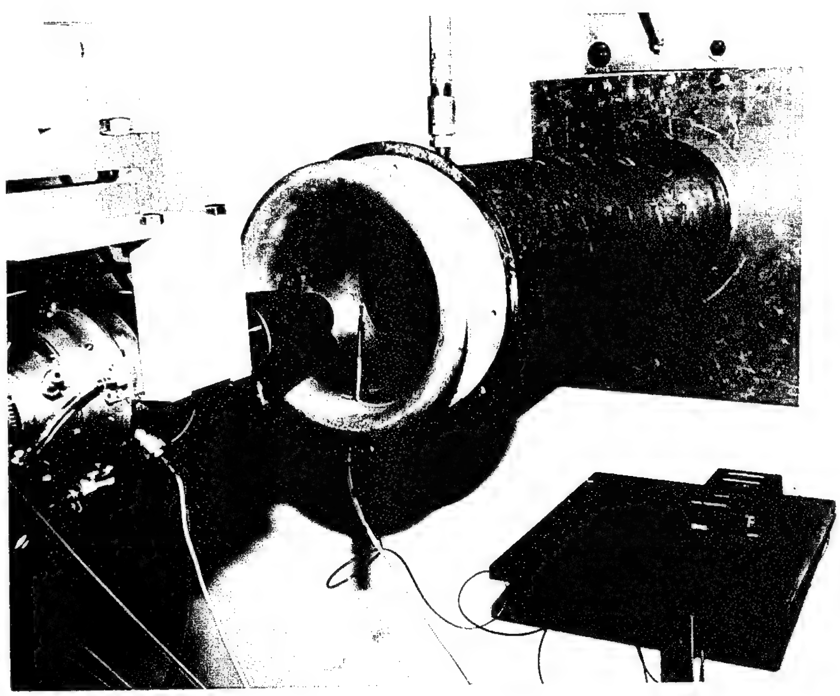

Figure 16 Temperature and Pressure Probe

5. JPX Pressure Gage

The manufacturer of the JPX-240 provided a pressure gage (0-1.6 bars) to control the operation of the engine. The gage was connected to an engine pressure port by flexible tubing. The pressure port sensed the static pressure between the impeller and the diffuser in the compressor section. The gage allowed verification of the idling and maximum pressure. Table 4 was provided by the manufacturer as a guide to start and operate the engine through its full range of RPM. No other measurement of RPM was made in the present program.

Pressure (bar)	RPM
1.15	49,000
0.2	57,000
0.4	79,000
0.5	83,000
0.6	92,000
0.7	95,000
0.8	102,000
0.9	105,000
1.0	110,000
1.1	112,000
1.15	115,000

Table 4 JPX Engine Operation Guide After Ref. [13]

D. DATA ACQUISITION

A schematic and a photograph of the data acquisition system are shown in Figures 17 and 18 respectively. The HP 9000 Series 300 workstation was used to control two data acquisition systems, and to store and process the data.

All measurements other than pressures were scanned using instruments addressed through the HP-IB (IEEE-488) bus. The strain-gage readings were scanned

using an HP 3497A Data Acquisition/Control Unit onto a HP digital multimeter. The fuel flow-meter frequency output was connected directly to an HP 5328A frequency counter.

The pressures were recorded using a Scanivalve ZOC-14 scanning system controlled by the HP9000 Series 300 workstation. Calibration of the ZOC was provided by the CALSYS 2000 calibration standard. A comprehensive guide to the system is given by Wendland. [Ref. 15]

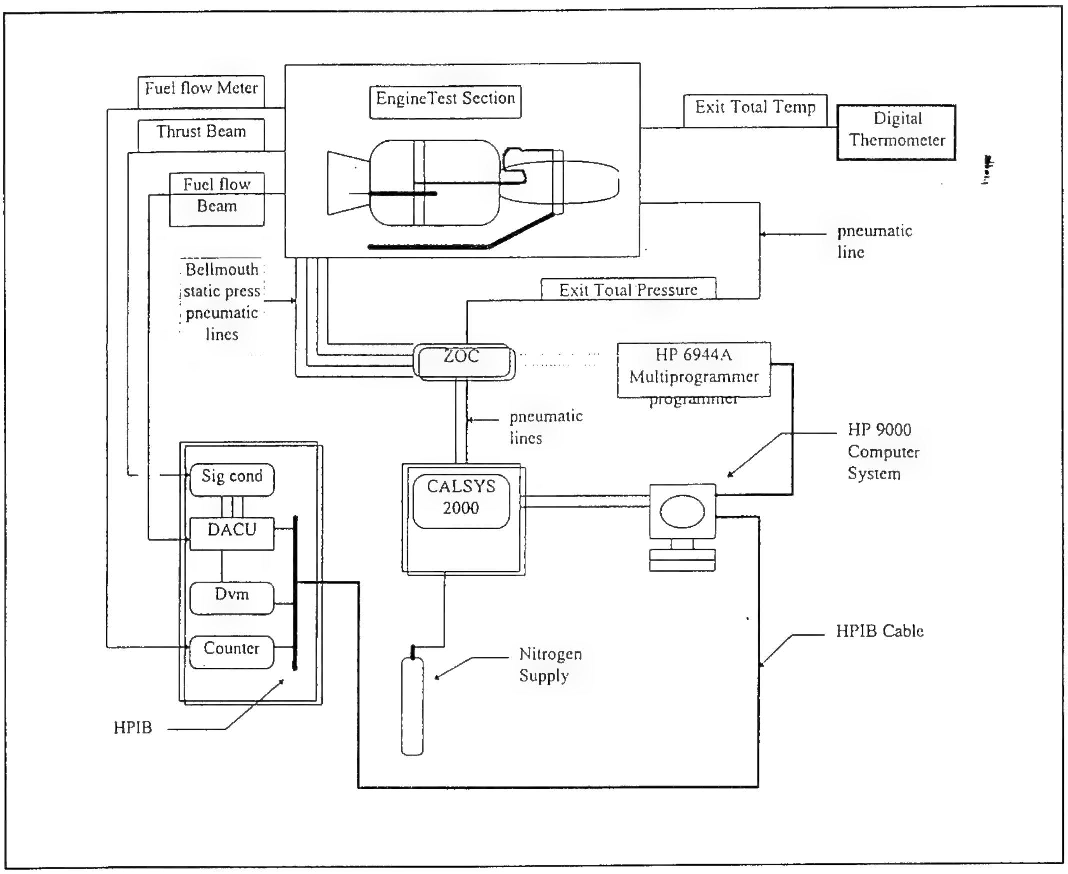

Figure 17 Data Acquisition System Schematic

Figure 18 Data Acquisition System

Program "SCAN_ZOC_08" was originally developed by Wendland to take pressure measurements from multiple ZOC's [Ref. 15]. This original program was modified in the present work (to "SCAN_ZOC_08_A") to "address" and collect samples from the HP-IB devices previously mentioned. The modifications to the program are given in Appendix C.

E. PROGRAM OF TESTS AND DATA OBTAINED

First, to verify the operation of the engine and to ensure that all measurements were obtained correctly, several preliminary engine test runs were conducted. The engine was operated for a series of 7 runs for a total span of 42 minutes. Secondly, a

series of 10 runs was performed at fixed compressor pressure levels to obtain performance data for the engine. In the second series, at each pressure setting, 3 to 8 data samples were taken at 30-second intervals over a 6 to 9 minute run. Because the (expected) RPM was given by the manufacturer at each tenth of a bar (Table 4), these particular pressures were used as set-points in the performance tests. The individual measurements obtained from multiple samples at fixed values of compressor pressure (throttle setting) are shown plotted in Figures 19 through 23. Each measurement will be discussed in turn in the following paragraphs. The multiple samples at each pressure setting were averaged in order to calculate the engine performance parameters given in the following section.

1. Air Flow Rate

Air flow-rate measurements are shown in Figure 19. Because of the high-speed sampling rate of the ZOC system, each of the four pressures from the bellmouth (and all other pressures) were sampled five times. This entire sampling sequence took less than one second. When the pressure data were reduced, the five samples for each port were averaged and then the four ports were averaged to get one throat static pressure for each (30 second) sample interval. This pressure was used in Equation 1 to calculate the flow rate. The data in Figure 19 show that at some pressure settings (1.15 bars), the repeatability from sample to sample was better than 1% . The largest total variation (15%) occurred at a setting of 0.7 bars. What was clear however, was that the variation occurred over time, from sample-to-sample and did not indicate lack of resolution in the measurements.

2. Fuel Flow Rate

Fuel flow-rate measurements are shown in Figure 20. Fuel flow rate as measured by the fuel flow-meter proved to be the most erratic measurement. The probable explanation for this was that two-phase flow occurred in the fuel line and flow

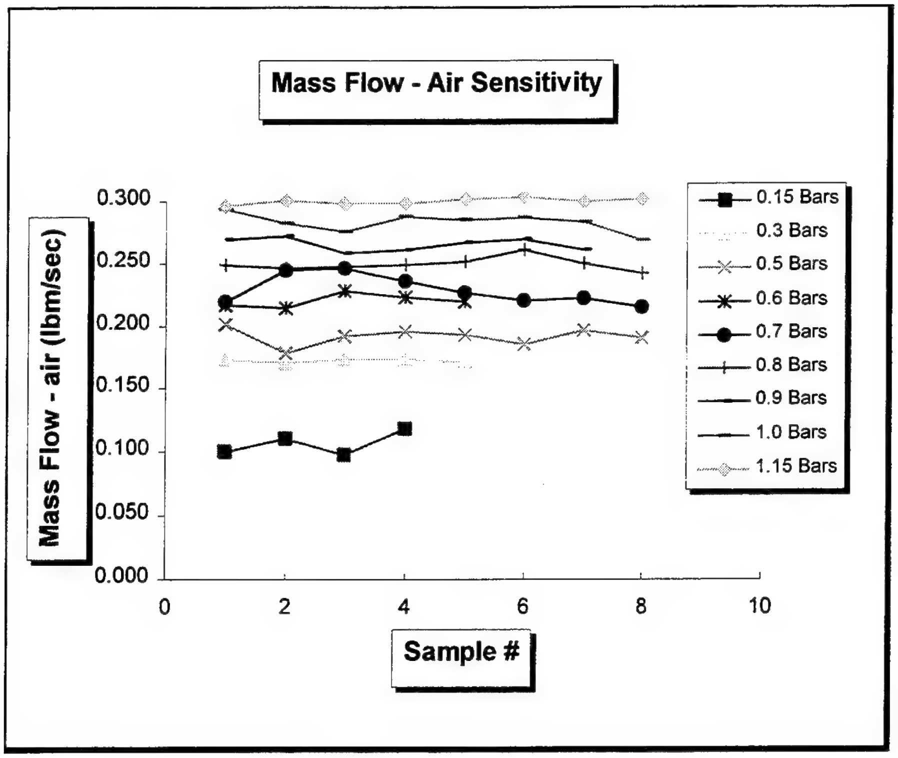

Figure 19 Air Mass Flow Measurements

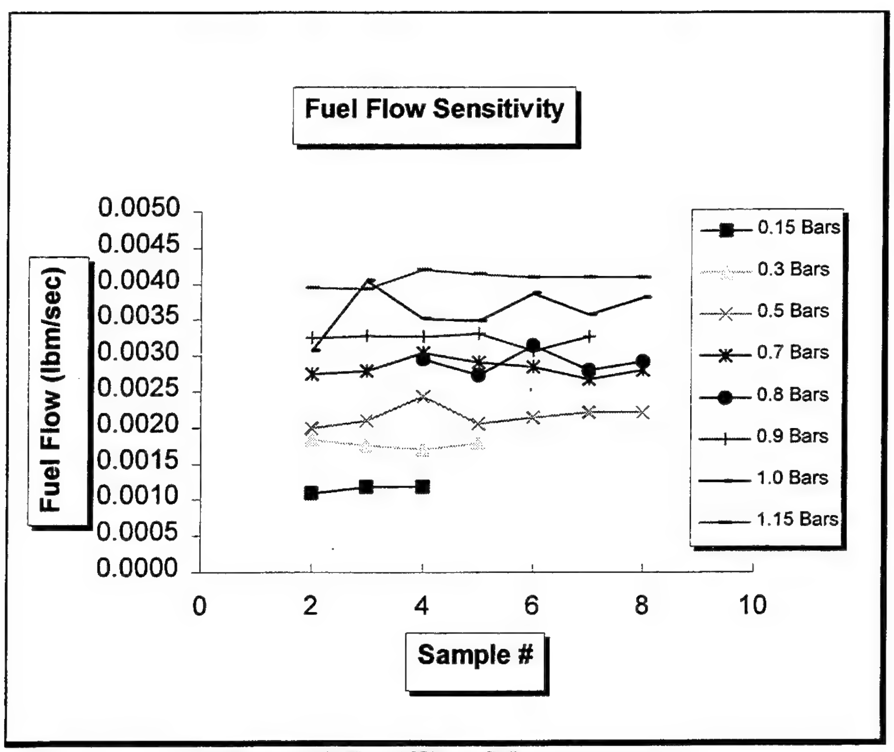

Figure 20 Fuel Flow Measurements

meter while operating the engine at the lower speeds. Not until the engine ran at its design RPM did the fuel flow-rate measurement appear to stabilize. However, some gas was always present in the fuel line.

3. Thrust

The thrust measurements are shown in Figure 21. The thrust proved to be the most stable of all the measurements. The behavior at the 0.7 bars pressure settings was the result of a manual throttle adjustment that was made after observing the pressure "creeping" autonomously during this particular run. This "creeping" would usually settle out after the engine was allowed to stabilize for a short period, prior to collecting the data.

4. Exit Stagnation Pressure

The exit stagnation pressure measurements are shown in Figure 22. The readings proved to be reasonably stable. These pressures were consistent with high speed, but not transonic flows. It is noted however that the probe was not at the nozzle exit plane but approximately 3 nozzle diameters downstream. Again, as with the thrust measurement at 0.7 bars, the pressure showed a steady rise and then dropped off to stabilize. The explanation for this behavior is the same as was given for the thrust measurement.

5. Exit Stagnation Temperature

Temperature measurement samples taken at each pressure (RPM) setting were very stable and consequently, in the plot of the measurements in Figure 23, each point is the average of all the samples taken at the indicated setting. Thus the variation in exit temperature with compressor pressure (or RPM) is seen clearly.

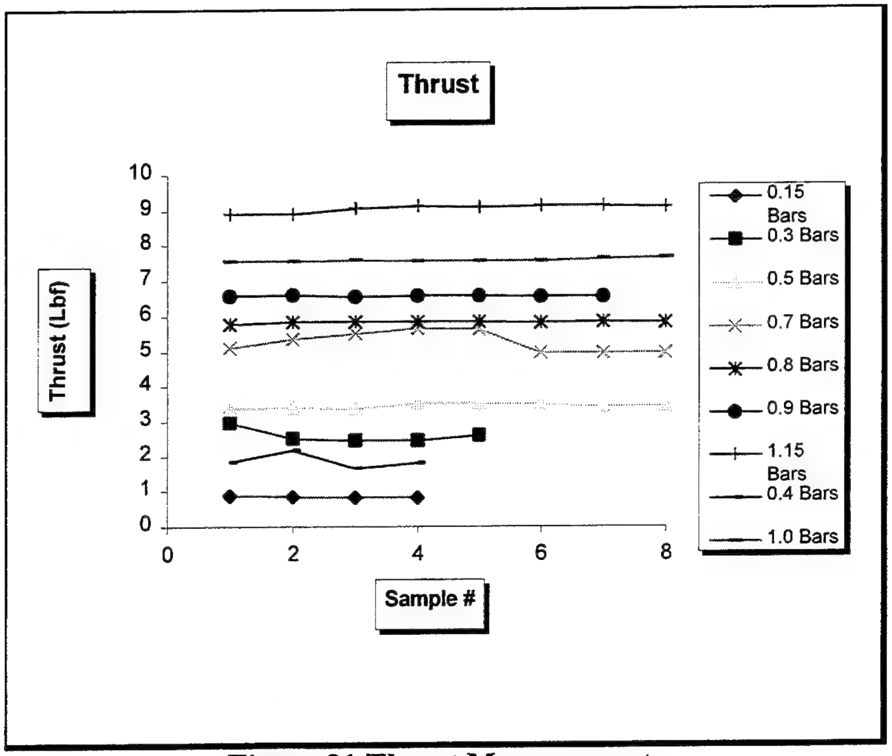

Figure 21 Thrust Measurements

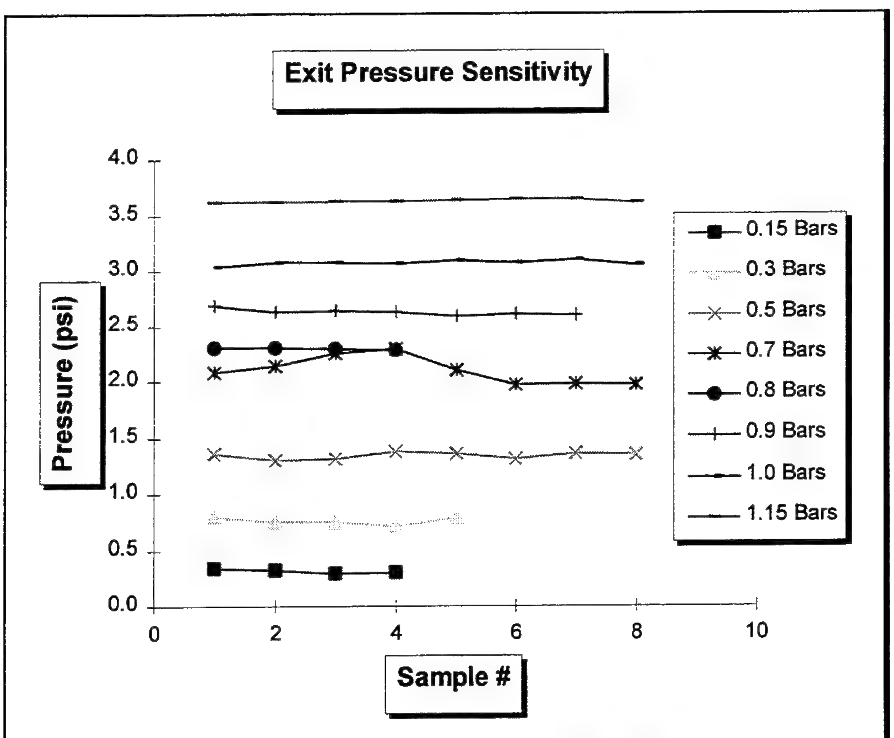

Figure 22 Exit Total Pressure Measurements

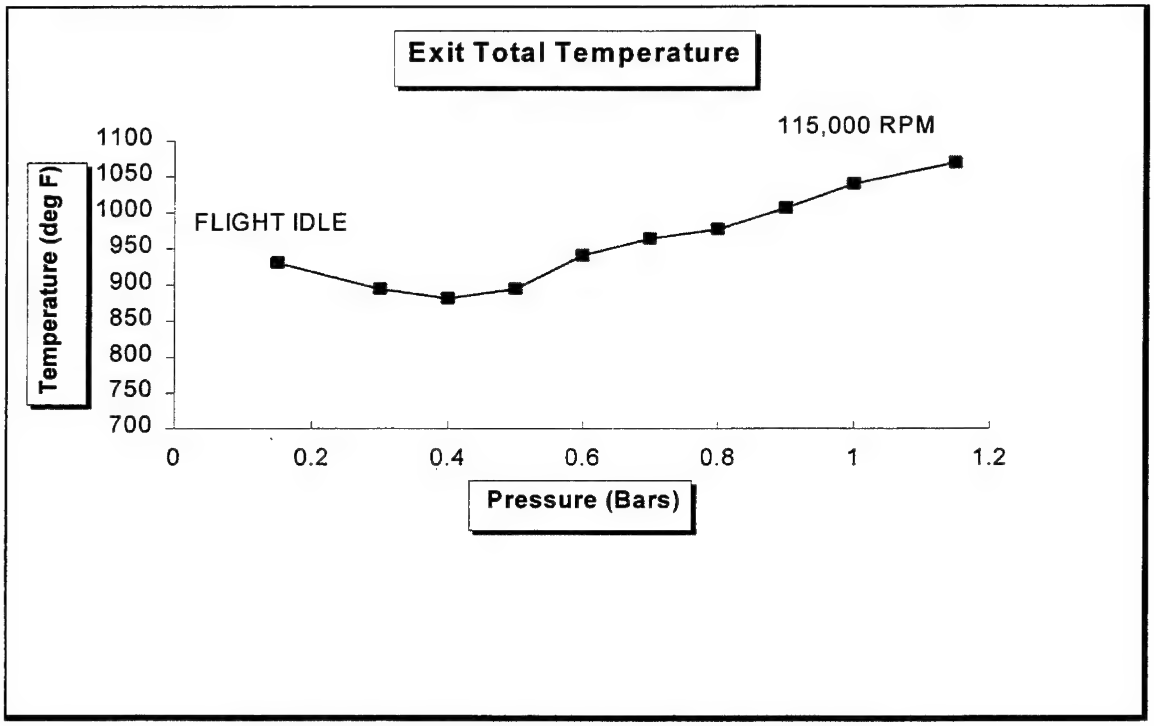

Figure 23 Exit Total Temperature Measurements

F. ENGINE PERFORMANCE

The calculated performance parameters for the engine (based on the average values of the samples taken at each pressure setting) are given in Table 5. The data collected at the design speed of the engine were in reasonable agreement with the specifications given by the manufacturer of the JPX-240. The SFC of the engine at design speed was measured to be approximately 10 % lower than the 1.806 lbm/lbf/hr specified. The data are shown plotted in Figure 24. As expected for a gas turbine running "off design", the performance was seen to drop off rapidly as the RPM decreased.

	Pressure		Fuel	Fuel	Mass	Temp	Pressure			
Test	JPX	Thrust	flow	flow	flow (air)	(exhaust)	(exhaust)		SFC	Sp Thrust
#	bars	lbf	lbm/sec	gpm	lbm/sec	deg F	inHg	psi	lb/lbf*hr	lbf/lb/sec
1	0.15	0.85	0.0012	0.016	0.108	931	0.64	0.31	4.97	8.08
2	0.3	1.84	0.0017	0.023	0.142	895	1.07	0.53	3.28	13.15
3	0.4	2.59	0.0018	0.025	0.173	883	1.55	0.76	2.55	15.00
4	0.5	3.44	0.0022	0.031	0.192	895	2.74	1.34	2.26	17.93
5	0.6	4.08	0.0024	0.033	0.220	941	3.17	1.56	2.09	18.54
6	0.7	5.26	0.0028	0.040	0.229	964	4.28	2.10	1.94	22.95
7	0.8	5.83	0.0029	0.041	0.250	960	4.71	2.31	1.80	23.31
8	0.9	6.56	0.0032	0.046	0.266	1006	5.35	2.63	1.78	24.69
9	1	7.57	0.0036	0.051	0.283	1040	6.26	3.07	1.73	26.76
10	1.15	9.04	0.0041	0.057	0.300	1070	7.39	3.63	1.62	30.13

Table 5 JPX-240 Test Results

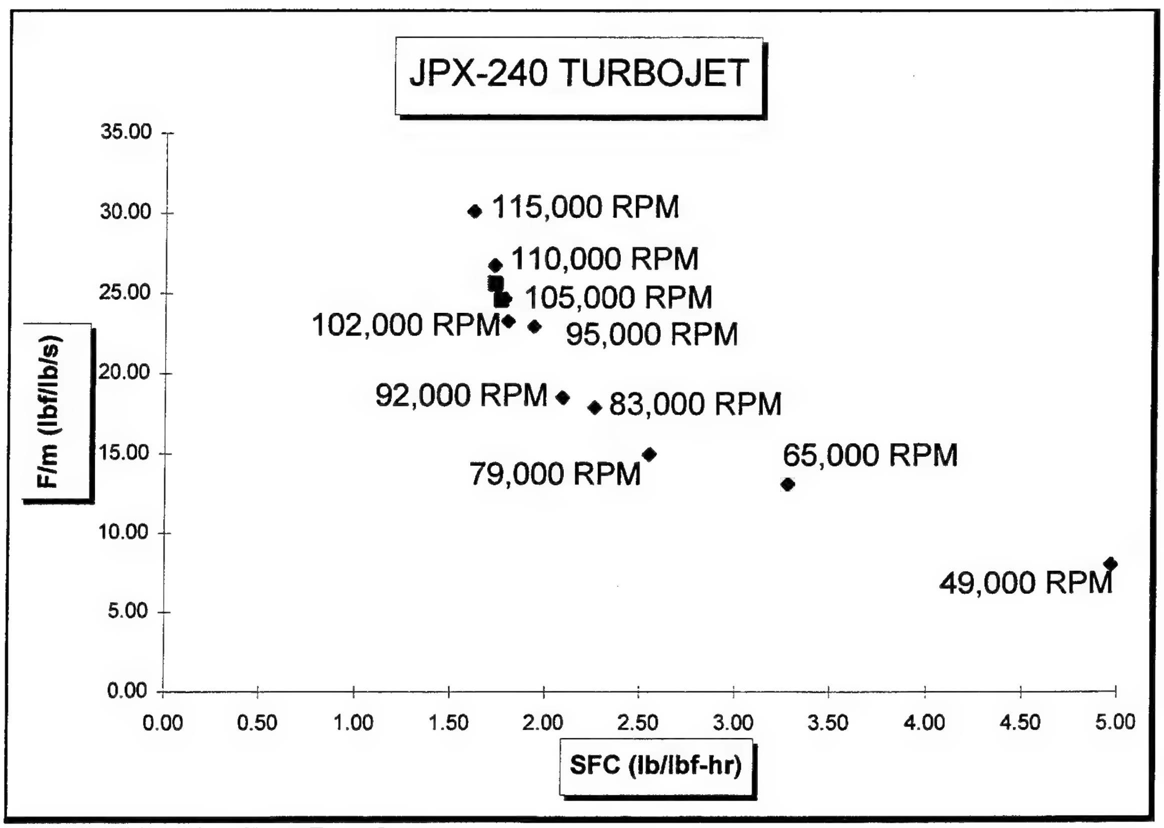

Figure 24 Engine Test Results

V. CODE SIMULATION OF MEASURED PERFORMANCE

The test program results for the design speed of 115,000 RPM were entered into *Gasturb* under the conditions that existed during the test, as shown in Table 6.

Mach #	Ambient Pressure (Pto)	Ambient Temperature (Tto)
0.0	14.78 psi	520.76 R

Table 6 Test Conditions

Gasturb required pressure ratio across the compressor and the losses across the stationary engine components to be input. The losses were not measured in the conduct of the tests, thus, the values had to be estimated. Because there was very little data on microturbines, references for larger engines were consulted. Aircraft Engine Design [Ref. 10] provided estimates for component losses in high performance engines. The compressor pressure ratio was provided by the engine manufacturer. The prescribed input values are given in Table 7. The remaining parameters required as inputs were burner exit temperature, compressor efficiency and turbine efficiency.

Compressor (πc)	Diffuser (πd)	Burner (πb)	Nozzle (πn)
2.13	98	.98	.98

Table 7 Required Pressure Ratio Inputs

In successive cycle calculations, the values of these three parameters were adjusted systematically until the code output matched the experimental results as

closely as possible. The best match was obtained with the values given in Table 8, and the results are given in Table 9. The code reproduced the measured behavior reasonably well considering the number of estimates that had to be made. The code-predicted values departed by as little as 3% to 4% from the measurements for all parameters that were compared.

Burner Exit Temperature(Tt4)	Compressor Efficiency (ηc)	Turbine Efficiency (ηt)
1685 R	0.72	0.75

Table 8 Iterated Parameters and Final Values

It is important to note that the exit temperature and pressure were taken at a fixed, single point. To properly evaluate the exit stagnation pressure and subsequently the exit velocity, the nozzle exit plane must be traversed and the measurements integrated and mass averaged. The stagnation pressure will then likely be closer to the code result. Since the probe was on the exhaust center-line, the single measurement would likely be larger than the mass-averaged value at the exit. This is supported by a comparison of the thrust that was measured and the thrust that was calculated assuming that the flow at the nozzle exit was uniform at the measured values of stagnation pressure and temperature, and with static pressure equal to ambient.

With these assumptions, the exit Mach number was calculated to be 0.57, the exit temperature was 1439° R and the exit-plane velocity (Ve) was 1096 ft/sec. The thrust [$T=(m_o + m_f)$ Ve] was then calculated to be 10.36 lb_f. This value exceeded the measurement by almost 15 %.

	EXPERIMENT	CODE
Pto (psi)	14.78	14.78 *
Tto (R)	520.67	520.67 *
m (lbm/sec)	.300	.300 *
mf (lbm/sec)	.0041	.0043
Thrust (lbf)	9.04	9.16
SFC (lbm/lbf/hr)	1.623	1.674
Specific Thrust (lbf/lbm/sec)	30.13	30.53
Exit Pressure, Pt9 (psi)	18.33	17.72
Exit Temp, Tt9 (deg F)	1070	1070.5
		* Specified Values

Table 9 Performance Comparison

VI. CODE PREDICTION OF TURBOPROP PERFORMANCE

As discussed in Section II, the turboprop provides a greater propulsive efficiency than the turbojet at lower flight speeds. To arrive at an equivalent horsepower for the JPX-240 that could be delivered to a gearbox and propeller, data from the turbojet cycle simulation were used as input to *Gasturb* as shown Table 10. A power turbine wheel (speed Np) was added to the cycle with an efficiency equivalent to that of the gas generator turbine wheel (speed Ng). The only additional parameter that *Gasturb* allowed to be varied was the exhaust-nozzle exit pressure, which was input as a pressure ratio. The closer the pressure ratio was to unity, the greater was the shaft-power output of the power turbine.

Turbine Inlet Temperature Tt4	1685 R
Turbine Exit Total Pressure Pt4a	18.83 psi
Turbine exit Total Temperature Tt4a	1530 R
Turbine Efficiency η_t	0.75
Compressor Efficiency η_c	0.72
Power Turbine Efficiency η_{pt}	0.75

Table 10 Performance Code Input

Since the code would not allow an exit pressure ratio of unity, a value of 1.001 was chosen, which resulted in a small residual thrust.

The results are shown in Table 11. The BSFC is seen to be quite high. However, the 5 horsepower delivered from the power turbine still must go through a gearbox to power the propeller, and inefficiencies will degrade the performance. A gearbox for such a small engine, to reduce the RPM from such high values would be relatively heavy, and this would reduce the overall specific weight (hp/lb) of the engine.

Shaft Horsepower Delivered to Gearbox PWSD	5 hp
Brake Specific Fuel Consumption BSFC	2.87 lbm/hp-hr
Residual Thrust FN	0.66 lbf

Table 11 Performance Code Output

VII. CONCLUSIONS AND RECOMMENDATIONS

A. CONCLUSIONS

A survey of existing full- and small-scale engines was conducted to determine the relative performances of different engine types, and their potential suitability for use in unmanned aerial vehicles. Spark ignition engines were found to dominate in applications requiring less than 400 horsepower. Relatively few turbojet engines were found with thrust levels below 700 lbs, although small gas-turbines have been the focus recently of DoD research and development efforts as a result of the UAV mission.

An engine rest rig was designed and built to evaluate the JPX-240 microturbine. The engine was successfully operated and data were collected over a range of engine RPM. The measured engine performance generally agreed with the manufacturer's specifications.

The engine performance code, *Gasturb*, modeled the microturbine cycle with reasonable results. *Gasturb* proved to be the best of three available codes to model the JPX cycle. The engine cycle performance code, *Thermoware*, demonstrated the increase in thermal efficiency gain through regenerative cycles. The greatest benefit of regeneration process was realized at the lower cycle pressure ratios and was seen to drop off with an increase in cycle pressure ratio and turbine inlet temperature.

Using test data for the JPX-240 obtained at the design RPM of 115,000, a code simulation was conducted, using estimated values of the efficiencies of the compressor and turbine, and of the combustion chamber exit temperature. The component efficiencies were critical to determining the feasibility of developing microturbines for UAV applications. The selected values were consistent with the levels of losses expected due to the adverse aerodynamic effects from reducing scale.

A turboprop simulation was evaluated by adding a power or 'free' turbine to the cycle with comparable losses to those established for the gas turbine. The shaft-power delivered was estimated to be 5 horsepower at a relatively high BSFC of 2.87 lbm/hp-hr. In addition to lower fuel consumption, the two-cycle engines available from most aircraft model companies give greater power-to-weight ratios for the same horsepower specified in the engine simulation.

B. RECOMMENDATIONS

All measurements taken from the JPX-240 to date were external to the motor. To obtain a more certain simulation of the small-engine cycle, combustion chamber temperature and pressure measurements should be taken.

The temperature and pressure taken at the exhaust nozzle exit were center-line values only. To accurately obtain the average temperature and pressure at the nozzle exit, a traverse of the exhaust flow must be made and the results mass-averaged.

The mass flow coefficient obtained from Reference 14 was close to unity. Calibration of the bellmouth with respect to a flat plate orifice would help verify the ASME design.

The fuel-flow strain-gage beam was constructed to facilitate the calibration of the fuel-flow meter; however, because the fuel flow was two-phase, the flow-meter provided inaccurate results. To obtain accurate measurements through the flow-meter, the two-phase flow of the propane must be maintained purely at the liquid state as required by the flow-meter specifications. A first step to correct this situation would be to keep the aluminum fuel tank fully pressurized at its initial state throughout the operation of the engine. This could be done by attaching a high pressure gas line to the release valve located at approximately the center of the tank. As the propane is released to the engine from the outlet end of the tank, it would remain in its liquid state as the volume of liquid propane decreases during the operation of the engine.

APPENDIX A. TEST RIG DRAWINGS

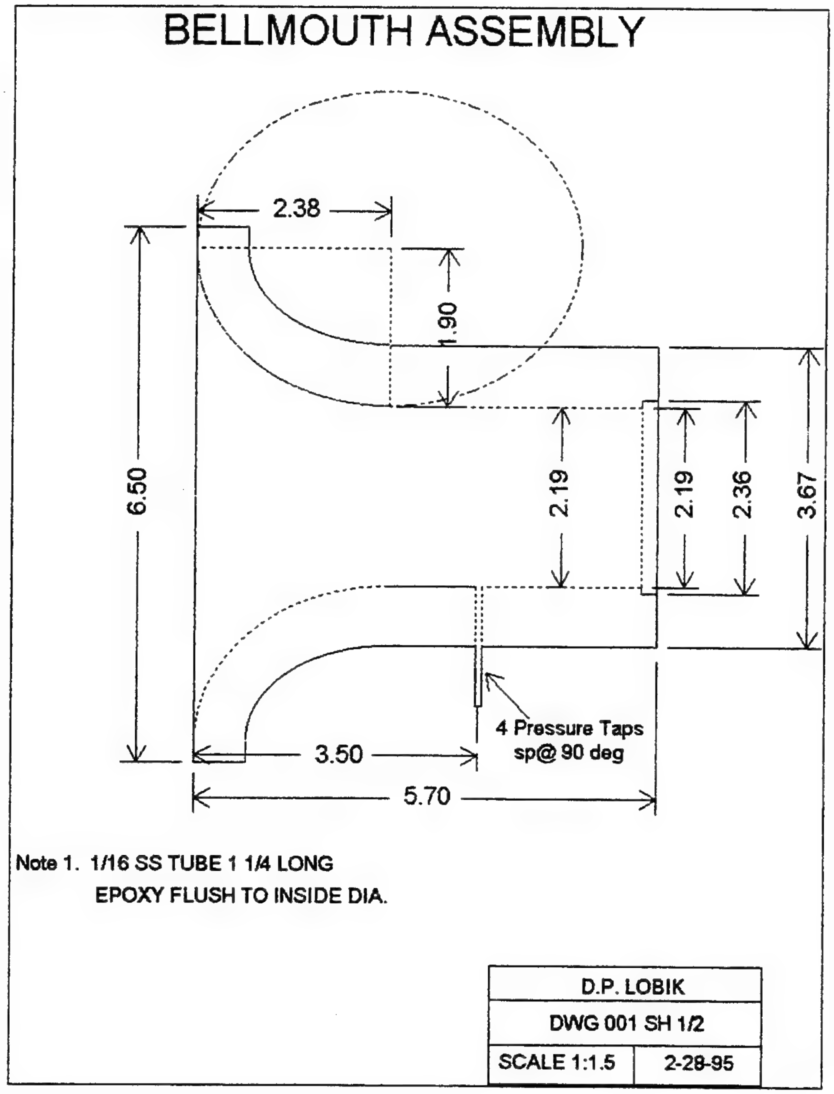

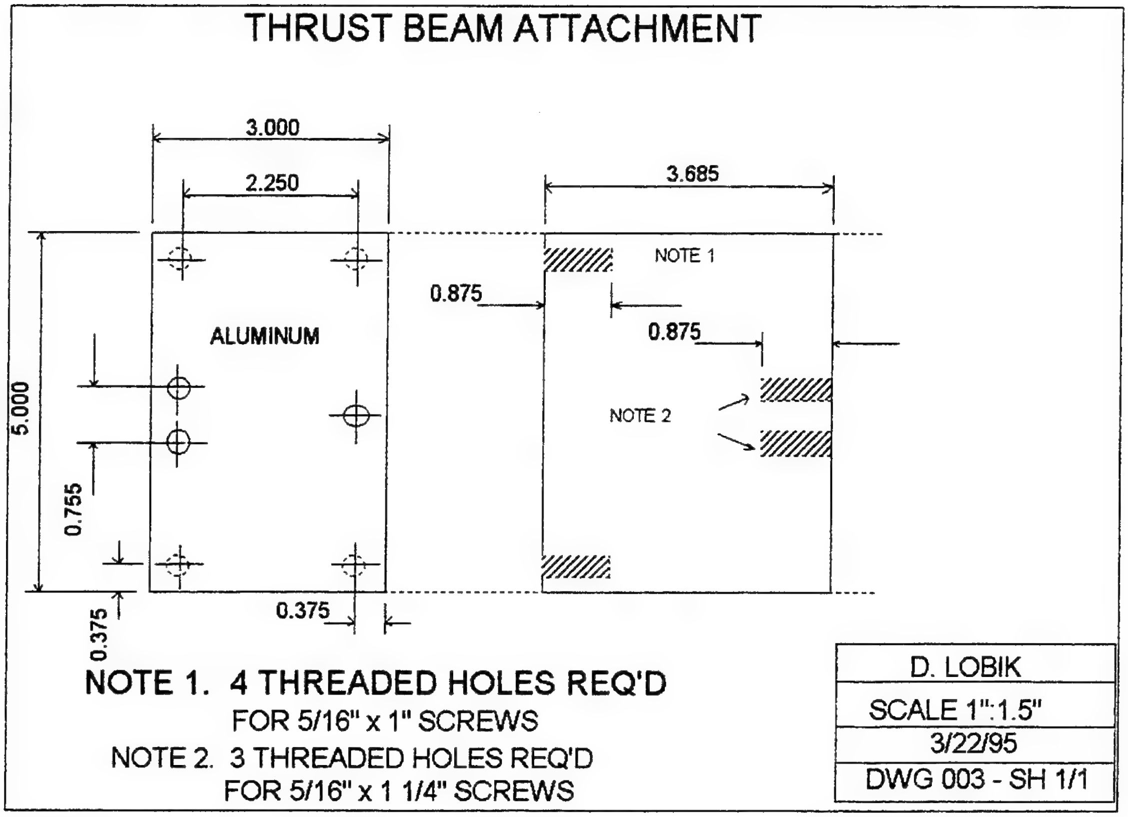
THRUST BEAM ATTACHMENT
3.000
2.250
3.685
NOTE 1
0.875
ALUMINUM
0.875
5.000
NOTE 2
0.755
0.375
0.375
NOTE 1. 4 THREADED HOLES REQ'D
FOR 5/16" x 1" SCREWS
NOTE 2. 3 THREADED HOLES REQ'D
FOR 5/16" x 1 1/4" SCREWS
D. LOBIK
SCALE 1":1.5"
3/22/95
DWG 003 - SH 1/1

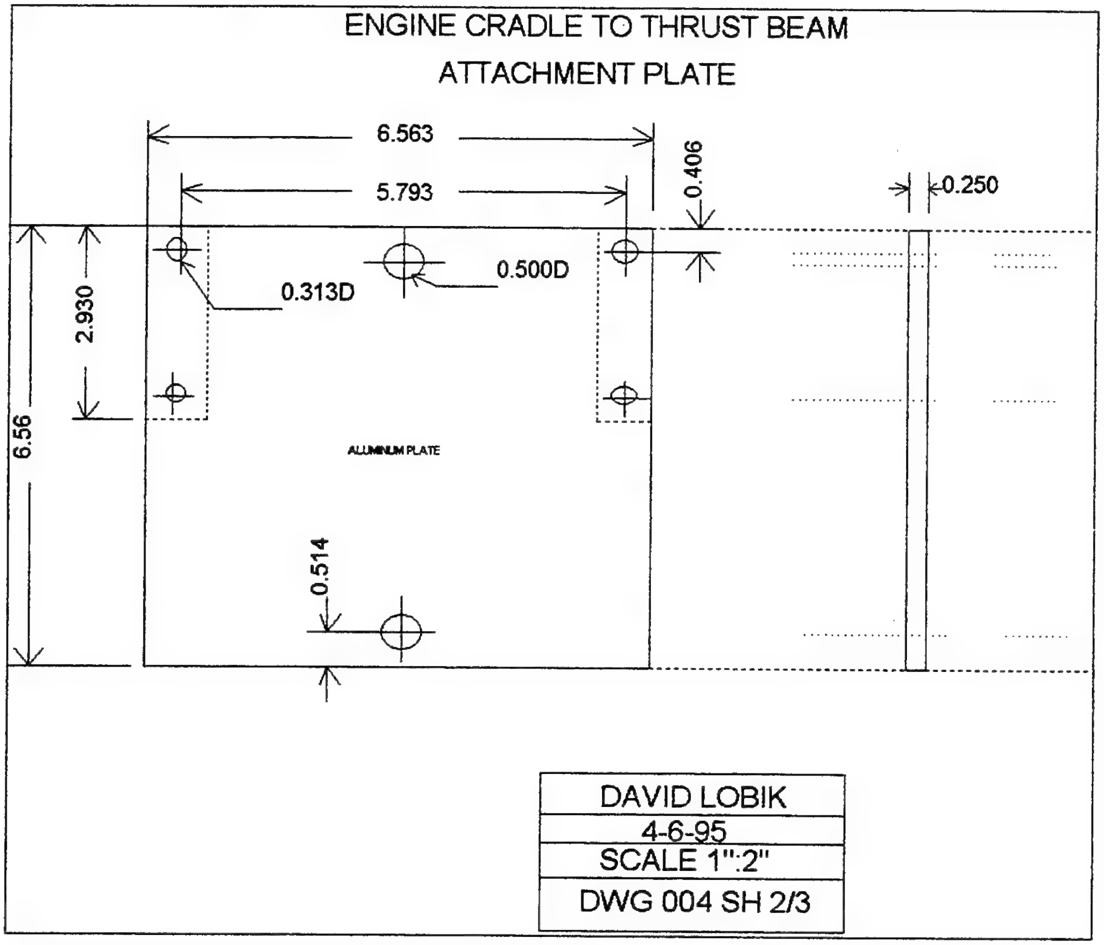

ENGINE CRADLE TO THRUST BEAM
ATTACHMENT PLATE
6.563
5.793
0.406
0.250
0.500D
0.313D
2.930
6.56
ALUMINUM PLATE
0.514
DAVID LOBIK
4-6-95
SCALE 1":2"
DWG 004 SH 2/3

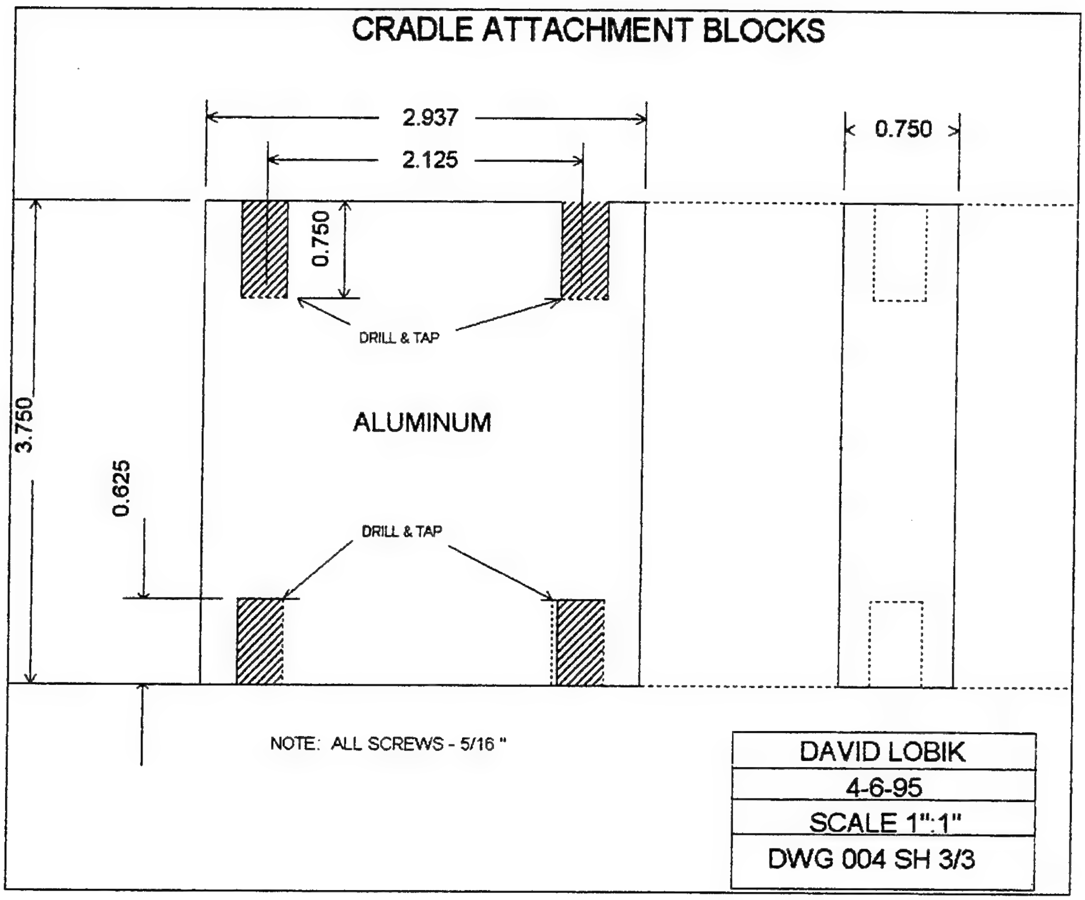
CRADLE ATTACHMENT BLOCKS
2.937
2.125
0.750
0.750
DRILL & TAP
ALUMINUM
3.750
0.625
DRILL & TAP
NOTE: ALL SCREWS - 5/16 "
DAVID LOBIK
4-6-95
SCALE 1":1"
DWG 004 SH 3/3

APPENDIX B. DATA REDUCTION

CALIBRATION CURVE FOR FUEL-FLOW STRAIN GAGE APPARATUS

UP		DOWN	
Volts	**Weight**	**Volts**	**Weight**
0.000055	0.335	0.000049	0.301
0.000248	1.52	0.000277	1.71
0.000308	1.88	0.000317	1.94
0.000405	2.48	0.000388	2.39
0.000479	2.94	0.000495	3.04
0.000565	3.47		

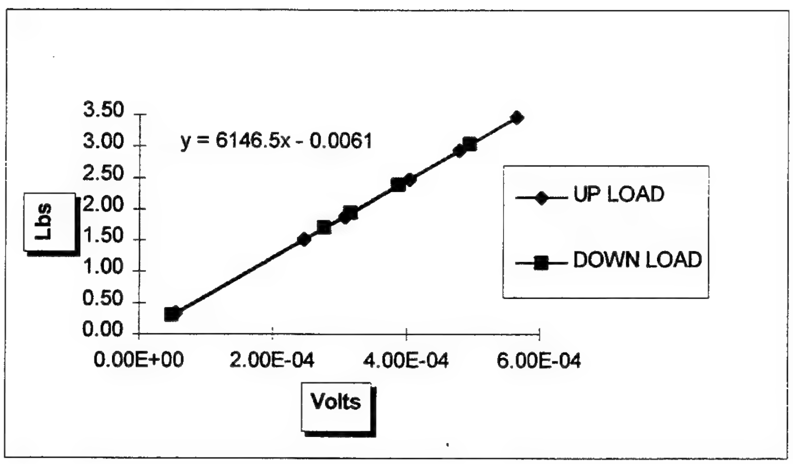

APPENDIX B1. STRAIN GAGE CALIBRATION

CALIBRATION FOR THRUST BEAM STRAIN GAGE APPARATUS

UP		DOWN	
Volts	**Lbs**	**Volts**	**Lbs**
0.000202	0.66	0.000275	0.661
0.000916	3.16	0.000562	1.66
0.001624	5.66	0.000988	3.16
0.002332	8.16	0.001271	4.16
0.003073	10.66	0.001699	5.66
0.003804	13.16	0.002402	8.16
0.005254	18.16	0.003107	10.66

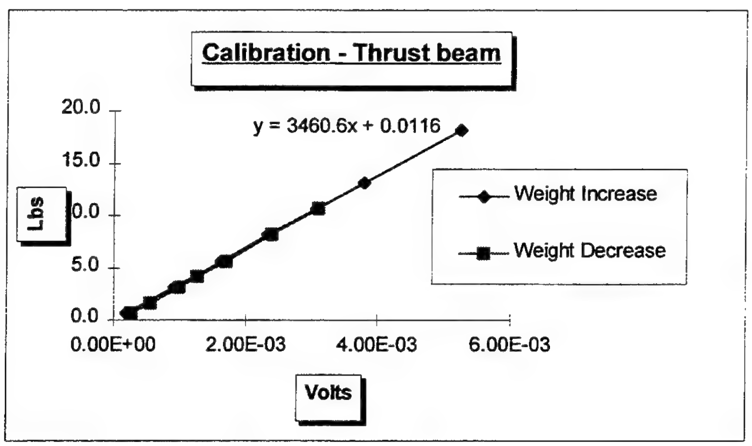

APPENDIX B2. THRUST BEAM CALIBRATION

APPENDIX C. ACQUISITION PROGRAM MODIFICATIONS

```
2030 !
2040 Collect_data:!~ COLLECT DATA ----------------------------------------
2050 IF Run=0 THEN
2060 PRINT "Program not initialized for data collection"
2070 DISP "Select F3 to initialize Set-up"
2080 GOTO Hold
2090 END IF
2100 CLEAR SCREEN
2110 !
2120 ! START THE DATA ACQUISITION LOOP TO TAKE SAMPLES FROM
2130 ! THE THRUST BEAM, FUEL FLOW METER, FUEL FLOW CALIBRATOR
2140 ! AND TEMP/PRESSURE PROBE.....
2150 !
2160 ! Fuel-flow strain gage output CHANNEL 0
2170  !
2180 Lbs_fuel_1=0
2190 FOR I=1 TO Iiter !START LOOP BASED ON # RUNS SPECIFIED
2200 CALL File(1)      !CREATE FILES FOR OUTPUT
2210 !
2220 !
2230 PRINT " Run # is"; TAB(10);Run
2240 Dacu=709
2250 Dvm=720
2260 D&r=705
2270 ASSIGN @Dcr TO Dcr
2280 ASSIGN @Dacu TO Dacu
2290 ASSIGN @DVM TO DVM
2300 !ASSIGN @6ages TO DVM,Dacu
2310 !CLEAR @Gages
2320 CLEAR @Dacu
2330 CLEAR @Dvm
2340 CLEAR @Dcr
2350 Ac$="AC"
2360 !
2370 ! Fuel-flow strain gage                    CHANNEL 0
2380 !
2390 Id$=VAL$(0)
2400 OUTPUT @Dacu;Ac$&Id$
2410    Total=0
2420    FOR J=1 TO 5
2430    OUTPUT @DVM ; " MEASURE:VOLT:DC? 1V"
2440    ENTER @DvM;Lbs_fuel
2450           Total=Total+Lbs_fuel+6926.61!calibration
2460 NEXT J
2470 !CLEAR @6ages
```

```
2480 Lbs_fuel=Total/5
2490 M-dot-fuel=(Lbs_fuel-Lbs_fuel-1)/(Xtime+20)
2500 Lbs_fuel_1=Lbs_fuel
2510 !
2520 !
2530 CLEAR @Dacu
2540 CLEAR @Dvm
2550 !
2550 ! Thrust beam output CHANNEL 5
2570 !
2580 CLEAR @Dacu
2590 CLEAR @Dvm
2600 Id$=VAL$(5)
2610 OUTPUT @Dacu:AC$&I d$
2620 Total=0 :
2630 FOR J=1 TO 5
2640 OUTPUT @Dvm;"MEASURE:VOLT:DC? 1V"
2650 ENTER @Dvm;Thrust
2660 Total=Total+Thrust*(-3460^559)
2670 NEXT J
2680 Thrust=Total/5
2685 !
2686 ! Take fuel flow reading fron Meter
2687 !
2690 !OUTPUT @Ocr;"PF4G7R n
2700 !OUTPUT @Dcr;"T"
2710 !ENTER @Dcr;Freq
2720 !PRINT "The Frequency for fuel flow meter is:";Freq;"Hz"
2730 PRINT "Thrust is ";TAB(27);Thrust;"lbs"
2740 PRINT "Fuel-flowis";T^B(25);M_dot_fuel;'lbs/sec orbiM_dot_fuel*.25205;"gpm"
2760 !
2770
2780 !
2790 !CLEAR @Gages
2800 CLEAR @Dacu
2810 CLEAR @Dcr
2820 CLEAR @DVM
2830 ASSIGN @Decu TO *
2840 ASSIGN @Dcr TO *
2850 ASSIGN @Dvm TO *
2860 !ASSIGN @Gages TO *
2870 PRINT
2880 PRINT "Collecting raw bellmouth pressure, exit, Thrust and FF data.'
2890 Count=Sample_number*32
2900
2910
2920 CALL Scan_zoc5( Count, Pulse )
                                    ! Set Count as function of sample number tand
                                    number of port readings (32)on ! Zoc for raw data
                                    collection.
                                    !Collect raw data into Memory 5ystem
2930 PRINT
2940 PRINT WRaw data collection complete."
```

```
2950 BEEP
2960 !
2970 Raw_data_xfer:!------ TRANSFER RAW DATA1 FM MEMORY SYSTEM TO HARD DISC
2980 PRINT
2990 !
3000 FOR Zoc_case=1 TO Zoc_number ! Collect raw data, reduee date and
3010      SELECT Zoc_case ! and store reduce data on hard drive
3070      CASE 1
3030      CALL Raw_dat(Buffer1,1)
3040      CASE 2
3050      IF Run>1 THEN
3060      Run=Run-1
3070      END IF
3080      CALL Raw_dat(Buffer2,2)
3090      CASE 3
3100      IF Run>1 THEN
3110      Run=Run-1
3120      END IF
3130      CALL Raw_dat(Buffer3,3)
3140      END SELECT
3150 NEXT Zoc_case
3160 !
3170 !PRINT "Xtime =";Xtime;"Iiter = ";I
3180 WAIT Xtime
3190 Run=Run+1
3200 NEXT I
3210 Run=Run-1
3230 !
```

APPENDIX D. ENGINE TEST DATA

JPX - 240 TEST RUN #1 DATA- 5 MAY 1995

	Engine	pressure	1.025 bars							
DATE	5/5/95									
Port #	Sample	Pamb-Ps inHg	Pamb-Ps psi	Tamb deg R	Pamb psi	R	Area ft^2	mass flow lbm/sec	Correction Factor C.F.	Corrected mass flow lbm/sec
1	1	-0.313	0.154	521	14.75	53.3	0.026		0.995	0.0000
	2	-0.313	0.154	521	14.75	53.3	0.026	0.273	0.995	0.2744
	3	-0.204	0.100	521	14.75	53.3	0.026	0.220	0.995	0.2214
	4	-0.368	0.181	521	14.75	53.3	0.026	0.296	0.995	0.2974
	5	-0.368	0.181	521	14.75	53.3	0.026	0.296	0.995	0.2974
	6	-0.204	0.100	521	14.75	53.3	0.026	0.220	0.995	0.2214
	7	-0.313	0.154	521	14.75	53.3	0.026	0.273	0.995	0.2744
	8	-0.258	0.127	521	14.75	53.3	0.026	0.248	0.995	0.2493
	9	-0.258	0.127	521	14.75	53.3	0.026	0.248	0.995	0.2493
	10	-0.313	0.154	521	14.75	53.3	0.026	0.273	0.995	0.2744
2	1	-0.192	0.095	521	14.75	53.3	0.026	0.214	0.995	0.2152
	2	-0.348	0.171	521	14.75	53.3	0.026	0.288	0.995	0.2896
	3	-0.348	0.171	521	14.75	53.3	0.026	0.288	0.995	0.2896
	4	-0.244	0.120	521	14.75	53.3	0.026	0.241	0.995	0.2425
	5	-0.296	0.146	521	14.75	53.3	0.026	0.266	0.995	0.2671
	6	-0.296	0.146	521	14.75	53.3	0.026	0.266	0.995	0.2671
	7	-0.296	0.146	521	14.75	53.3	0.026	0.266	0.995	0.2671
	8	-0.348	0.171	521	14.75	53.3	0.026	0.288	0.995	0.2896
	9	-0.348	0.171	521	14.75	53.3	0.026	0.288	0.995	0.2896
	10	-0.348	0.171	521	14.75	53.3	0.026	0.288	0.995	0.2896
3	1	-0.321	0.158	521	14.75	53.3	0.026	0.276	0.995	0.2779
	2	-0.147	0.072	521	14.75	53.3	0.026	0.187	0.995	0.1880
	3	-0.321	0.158	521	14.75	53.3	0.026	0.276	0.995	0.2779
	4	-0.321	0.158	521	14.75	53.3	0.026	0.276	0.995	0.2779
	5	-0.205	0.101	521	14.75	53.3	0.026	0.221	0.995	0.2221
	6	-0.321	0.158	521	14.75	53.3	0.026	0.276	0.995	0.2779
	7	-0.321	0.158	521	14.75	53.3	0.026	0.276	0.995	0.2779
	8	-0.263	0.129	521	14.75	53.3	0.026	0.250	0.995	0.2515
	9	-0.321	0.158	521	14.75	53.3	0.026	0.276	0.995	0.2779
	10	-0.379	0.186	521	14.75	53.3	0.026	0.300	0.995	0.3019

4	1	-0.326	0.160	521	14.75	53.3	0.026	0.279	0.995	0.2800
	2	-0.326	0.160	521	14.75	53.3	0.026	0.279	0.995	0.2800
	3	-0.128	0.063	521	14.75	53.3	0.026	0.175	0.995	0.1758
	4	-0.326	0.160	521	14.75	53.3	0.026	0.279	0.995	0.2800
	5	-0.326	0.160	521	14.75	53.3	0.026	0.279	0.995	0.2800
	6	-0.194	0.095	521	14.75	53.3	0.026	0.215	0.995	0.2162
	7	-0.326	0.160	521	14.75	53.3	0.026	0.279	0.995	0.2800
	8	-0.326	0.160	521	14.75	53.3	0.026	0.279	0.995	0.2800
	9	-0.260	0.128	521	14.75	53.3	0.026	0.249	0.995	0.2501
	10	-0.392	0.192	521	14.75	53.3	0.026	0.305	0.995	0.3070
									average	**0.2582**

Engine Run #2 - 23 MAY 1996

Date	Pressure									
5/23/95	.81 bars									
Run #1									Correction	Corrected
Port #	Sample	Pressure	Pamb-Ps	Tamb	Pamb	R	Area	mass flow	Factor	mass flow
		inHg	psi	deg R	psi		ft^2	lbm/sec	CF	lbm/sec
1	1	-0.270	0.132	520	14.72	53.3	0.026	0.253	0.995	0.255
	2	-0.270	0.132	520	14.72	53.3	0.026	0.253	0.995	0.255
	3	-0.324	0.159	520	14.72	53.3	0.026	0.278	0.995	0.279
	4	-0.215	0.106	520	14.72	53.3	0.026	0.226	0.995	0.227
	5	-0.270	0.132	520	14.72	53.3	0.026	0.253	0.995	0.255
2	1	-0.228	0.112	520	14.72	53.3	0.026	0.233	0.995	0.234
	2	-0.228	0.112	520	14.72	53.3	0.026	0.233	0.995	0.234
	3	-0.332	0.163	520	14.72	53.3	0.026	0.281	0.995	0.283
	4	-0.280	0.138	520	14.72	53.3	0.026	0.258	0.995	0.260
	5	-0.176	0.087	520	14.72	53.3	0.026	0.205	0.995	0.206
3	1	-0.075	0.037	520	14.72	53.3	0.026	0.134	0.995	0.134
	2	-0.191	0.094	520	14.72	53.3	0.026	0.213	0.995	0.215
	3	-0.133	0.065	520	14.72	53.3	0.026	0.178	0.995	0.179
	4	-0.308	0.151	520	14.72	53.3	0.026	0.271	0.995	0.272
	5	-0.308	0.151	520	14.72	53.3	0.026	0.271	0.995	0.272
4	1	-0.351	0.172	520	14.72	53.3	0.026	0.289	0.995	0.291
	2	-0.219	0.108	520	14.72	53.3	0.026	0.228	0.995	0.230
	3	-0.351	0.172	520	14.72	53.3	0.026	0.289	0.995	0.291
	4	-0.153	0.075	520	14.72	53.3	0.026	0.191	0.995	0.192
	5	-0.351	0.172	520	14.72	53.3	0.026	0.289	0.995	0.291
Run #2										
1	1	-0.379	0.186	520	14.72	53.3	0.026	0.300	0.995	0.302
	2	-0.270	0.132	520	14.72	53.3	0.026	0.253	0.995	0.255
	3	-0.324	0.159	520	14.72	53.3	0.026	0.278	0.995	0.279
	4	-0.215	0.106	520	14.72	53.3	0.026	0.226	0.995	0.227
	5	-0.270	0.132	520	14.72	53.3	0.026	0.253	0.995	0.255
2	1	-0.333	0.164	520	14.72	53.3	0.026	0.282	0.995	0.283
	2	-0.176	0.087	520	14.72	53.3	0.026	0.205	0.995	0.206
	3	-0.228	0.112	520	14.72	53.3	0.026	0.233	0.995	0.234
	4	-0.228	0.112	520	14.72	53.3	0.026	0.233	0.995	0.234
	5	-0.280	0.138	520	14.72	53.3	0.026	0.258	0.995	0.260
3	1	-0.133	0.065	520	14.72	53.3	0.026	0.178	0.995	0.179
	2	-0.249	0.123	520	14.72	53.3	0.026	0.244	0.995	0.245
	3	-0.133	0.065	520	14.72	53.3	0.026	0.178	0.995	0.179
	4	-0.249	0.123	520	14.72	53.3	0.026	0.244	0.995	0.245
	5	-0.075	0.037	520	14.72	53.3	0.026	0.134	0.995	0.134
4	1	-0.417	0.205	520	14.72	53.3	0.026	0.315	0.995	0.317
	2	-0.219	0.108	520	14.72	53.3	0.026	0.228	0.995	0.230
	3	-0.351	0.172	520	14.72	53.3	0.026	0.289	0.995	0.291
	4	-0.219	0.108	520	14.72	53.3	0.026	0.228	0.995	0.230
	5	-0.285	0.140	520	14.72	53.3	0.026	0.261	0.995	0.262

Run #3										
1	1	-0.160	0.079	520	14.72	53.3	0.026	0.195	0.995	0.196
	2	-0.324	0.159	520	14.72	53.3	0.026	0.278	0.995	0.279
	3	-0.160	0.079	520	14.72	53.3	0.026	0.195	0.995	0.196
	4	-0.324	0.159	520	14.72	53.3	0.026	0.278	0.995	0.279
	5	-0.215	0.106	520	14.72	53.3	0.026	0.226	0.995	0.227
2	1	-0.280	0.138	520	14.72	53.3	0.026	0.258	0.995	0.260
	2	-0.176	0.087	520	14.72	53.3	0.026	0.205	0.995	0.206
	3	-0.280	0.138	520	14.72	53.3	0.026	0.258	0.995	0.260
	4	-0.124	0.061	520	14.72	53.3	0.026	0.172	0.995	0.173
	5	-0.176	0.087	520	14.72	53.3	0.026	0.205	0.995	0.206
3	1	-0.308	0.151	520	14.72	53.3	0.026	0.271	0.995	0.272
	2	-0.191	0.094	520	14.72	53.3	0.026	0.213	0.995	0.215
	3	-0.191	0.094	520	14.72	53.3	0.026	0.213	0.995	0.215
	4	-0.249	0.123	520	14.72	53.3	0.026	0.244	0.995	0.245
	5	-0.191	0.094	520	14.72	53.3	0.026	0.213	0.995	0.215
4	1	-0.087	0.043	520	14.72	53.3	0.026	0.144	0.995	0.145
	2	-0.219	0.108	520	14.72	53.3	0.026	0.228	0.995	0.230
	3	-0.351	0.172	520	14.72	53.3	0.026	0.289	0.995	0.291
	4	-0.285	0.140	520	14.72	53.3	0.026	0.261	0.995	0.262
	5	-0.417	0.205	520	14.72	53.3	0.026	0.315	0.995	0.317
Run #4										
1	1	-0.270	0.132	520	14.72	53.3	0.026	0.253	0.995	0.255
	2	-0.160	0.079	520	14.72	53.3	0.026	0.195	0.995	0.196
	3	-0.324	0.159	520	14.72	53.3	0.026	0.278	0.995	0.279
	4	-0.270	0.132	520	14.72	53.3	0.026	0.253	0.995	0.255
	5	-0.379	0.186	520	14.72	53.3	0.026	0.300	0.995	0.302
2	1	-0.124	0.061	520	14.72	53.3	0.026	0.172	0.995	0.173
	2	-0.280	0.138	520	14.72	53.3	0.026	0.258	0.995	0.260
	3	-0.124	0.061	520	14.72	53.3	0.026	0.172	0.995	0.173
	4	-0.280	0.138	520	14.72	53.3	0.026	0.258	0.995	0.260
	5	-0.072	0.035	520	14.72	53.3	0.026	0.131	0.995	0.132
3	1	-0.249	0.123	520	14.72	53.3	0.026	0.244	0.995	0.245
	2	-0.191	0.094	520	14.72	53.3	0.026	0.213	0.995	0.215
	3	-0.249	0.123	520	14.72	53.3	0.026	0.244	0.995	0.245
	4	-0.133	0.065	520	14.72	53.3	0.026	0.178	0.995	0.179
	5	-0.191	0.094	520	14.72	53.3	0.026	0.213	0.995	0.215
4	1	-0.417	0.205	520	14.72	53.3	0.026	0.315	0.995	0.317
	2	-0.285	0.140	520	14.72	53.3	0.026	0.261	0.995	0.262
	3	-0.351	0.172	520	14.72	53.3	0.026	0.289	0.995	0.291
	4	-0.351	0.172	520	14.72	53.3	0.026	0.289	0.995	0.291
	5	-0.285	0.140	520	14.72	53.3	0.026	0.261	0.995	0.262

Run #5										
1	1	-0.160	0.079	520	14.72	53.3	0.026	0.195	0.995	0.196
	2	-0.270	0.132	520	14.72	53.3	0.026	0.253	0.995	0.255
	3	-0.106	0.052	520	14.72	53.3	0.026	0.159	0.995	0.159
	4	-0.270	0.132	520	14.72	53.3	0.026	0.253	0.995	0.255
	5	-0.270	0.132	520	14.72	53.3	0.026	0.253	0.995	0.255
2	1	-0.332	0.163	520	14.72	53.3	0.026	0.281	0.995	0.283
	2	-0.176	0.087	520	14.72	53.3	0.026	0.205	0.995	0.206
	3	-0.228	0.112	520	14.72	53.3	0.026	0.233	0.995	0.234
	4	-0.124	0.061	520	14.72	53.3	0.026	0.172	0.995	0.173
	5	-0.280	0.138	520	14.72	53.3	0.026	0.258	0.995	0.260
3	1	-0.249	0.123	520	14.72	53.3	0.026	0.244	0.995	0.245
	2	-0.308	0.151	520	14.72	53.3	0.026	0.271	0.995	0.272
	3	-0.249	0.123	520	14.72	53.3	0.026	0.244	0.995	0.245
	4	-0.249	0.123	520	14.72	53.3	0.026	0.244	0.995	0.245
	5	-0.075	0.037	520	14.72	53.3	0.026	0.134	0.995	0.134
4	1	-0.087	0.043	520	14.72	53.3	0.026	0.144	0.995	0.145
	2	-0.351	0.172	520	14.72	53.3	0.026	0.289	0.995	0.291
	3	-0.351	0.172	520	14.72	53.3	0.026	0.289	0.995	0.291
	4	-0.483	0.237	520	14.72	53.3	0.026	0.339	0.995	0.341
	5	-0.351	0.172	520	14.72	53.3	0.026	0.289	0.995	0.291
Run #6										
1	1	-0.160	0.079	520	14.72	53.3	0.026	0.195	0.995	0.196
	2	-0.270	0.132	520	14.72	53.3	0.026	0.253	0.995	0.255
	3	-0.160	0.079	520	14.72	53.3	0.026	0.195	0.995	0.196
	4	-0.270	0.132	520	14.72	53.3	0.026	0.253	0.995	0.255
	5	-0.215	0.106	520	14.72	53.3	0.026	0.226	0.995	0.227
2	1	-0.280	0.138	520	14.72	53.3	0.026	0.258	0.995	0.260
	2	-0.176	0.087	520	14.72	53.3	0.026	0.205	0.995	0.206
	3	-0.228	0.112	520	14.72	53.3	0.026	0.233	0.995	0.234
	4	-0.124	0.061	520	14.72	53.3	0.026	0.172	0.995	0.173
	5	-0.228	0.112	520	14.72	53.3	0.026	0.233	0.995	0.234
3	1	-0.249	0.123	520	14.72	53.3	0.026	0.244	0.995	0.245
	2	-0.249	0.123	520	14.72	53.3	0.026	0.244	0.995	0.245
	3	-0.191	0.094	520	14.72	53.3	0.026	0.213	0.995	0.215
	4	-0.249	0.123	520	14.72	53.3	0.026	0.244	0.995	0.245
	5	-0.191	0.094	520	14.72	53.3	0.026	0.213	0.995	0.215
4	1	-0.219	0.108	520	14.72	53.3	0.026	0.228	0.995	0.230
	2	-0.351	0.172	520	14.72	53.3	0.026	0.289	0.995	0.291
	3	-0.351	0.172	520	14.72	53.3	0.026	0.289	0.995	0.291
	4	-0.351	0.172	520	14.72	53.3	0.026	0.289	0.995	0.291
	5	-0.351	0.172	520	14.72	53.3	0.026	0.289	0.995	0.291

Run #7										
1	1	-0.324	0.159	520	14.72	53.3	0.026	0.278	0.995	0.279
	2	-0.160	0.079	520	14.72	53.3	0.026	0.195	0.995	0.196
	3	-0.270	0.132	520	14.72	53.3	0.026	0.253	0.995	0.255
	4	-0.324	0.159	520	14.72	53.3	0.026	0.278	0.995	0.279
	5	-0.270	0.132	520	14.72	53.3	0.026	0.253	0.995	0.255
	1	-0.124	0.061	520	14.72	53.3	0.026	0.172	0.995	0.173
2	2	-0.280	0.138	520	14.72	53.3	0.026	0.258	0.995	0.260
	3	-0.072	0.035	520	14.72	53.3	0.026	0.131	0.995	0.132
	4	-0.228	0.112	520	14.72	53.3	0.026	0.233	0.995	0.234
	5	-0.072	0.035	520	14.72	53.3	0.026	0.131	0.995	0.132
	1	-0.249	0.123	520	14.72	53.3	0.026	0.244	0.995	0.245
3	2	-0.191	0.094	520	14.72	53.3	0.026	0.213	0.995	0.215
	3	-0.249	0.123	520	14.72	53.3	0.026	0.244	0.995	0.245
	4	-0.133	0.065	520	14.72	53.3	0.026	0.178	0.995	0.179
	5	-0.249	0.123	520	14.72	53.3	0.026	0.244	0.995	0.245
	1	-0.351	0.172	520	14.72	53.3	0.026	0.289	0.995	0.291
4	2	-0.285	0.140	520	14.72	53.3	0.026	0.261	0.995	0.262
	3	-0.285	0.140	520	14.72	53.3	0.026	0.261	0.995	0.262
	4	-0.351	0.172	520	14.72	53.3	0.026	0.289	0.995	0.291
	5	-0.219	0.108	520	14.72	53.3	0.026	0.228	0.995	0.230
Run #8										
	1	-0.270	0.132	520	14.72	53.3	0.026	0.253	0.995	0.255
	2	-0.215	0.106	520	14.72	53.3	0.026	0.226	0.995	0.227
1	3	-0.324	0.159	520	14.72	53.3	0.026	0.278	0.995	0.279
	4	-0.160	0.079	520	14.72	53.3	0.026	0.195	0.995	0.196
	5	-0.270	0.132	520	14.72	53.3	0.026	0.253	0.995	0.255
	1	-0.228	0.112	520	14.72	53.3	0.026	0.233	0.995	0.234
	2	-0.176	0.087	520	14.72	53.3	0.026	0.205	0.995	0.206
2	3	-0.332	0.163	520	14.72	53.3	0.026	0.281	0.995	0.283
	4	-0.228	0.112	520	14.72	53.3	0.026	0.233	0.995	0.234
	5	-0.280	0.138	520	14.72	53.3	0.026	0.258	0.995	0.260
	1	-0.191	0.094	520	14.72	53.3	0.026	0.213	0.995	0.215
	2	-0.308	0.151	520	14.72	53.3	0.026	0.271	0.995	0.272
3	3	-0.017	0.008	520	14.72	53.3	0.026	0.064	0.995	0.064
	4	-0.308	0.151	520	14.72	53.3	0.026	0.271	0.995	0.272
	5	-0.133	0.065	520	14.72	53.3	0.026	0.178	0.995	0.179
	1	-0.351	0.172	520	14.72	53.3	0.026	0.289	0.995	0.291
	2	-0.285	0.140	520	14.72	53.3	0.026	0.261	0.995	0.262
4	3	-0.351	0.172	520	14.72	53.3	0.026	0.289	0.995	0.291
	4	-0.285	0.140	520	14.72	53.3	0.026	0.261	0.995	0.262
	5	-0.351	0.172	520	14.72	53.3	0.026	0.289	0.995	0.291
									average	0.239

		Date		Pressure			
		5/23/95		.81 bars			
Run #	Thrust lbf	Air mass flow lbm/sec	Fuel mass flow lbm/sec	mass flow gpm	Fuel flow volts	SFC lb/lbf*hr	Specific Thrust lbf/lb/sec
1	5.733	0.249			4.630		
2	5.6	0.249	0.0027	0.038	4.670	1.736	22.49
3	5.72	0.240	0.0028	0.039	4.662	1.756	23.83
4	5.75	0.246	0.0030	0.043	4.658	1.898	23.37
5	5.78	0.245	0.0029	0.041	4.673	1.801	23.59
6	5.75	0.246	0.0028	0.040	4.675	1.758	23.37
7	5.52	0.239	0.0029	0.041	4.681	1.904	23.10
8	5.81	0.248	0.0028	0.039	4.660	1.716	23.43
average	5.71	0.245	0.0028	0.040	4.668	1.796	23.31

JPX Run MAY 27

Run #	Press	Thrust	Fuel flow	Fuel flow	corrected Mass flow (air)	Fuel Flow Meter	Total Temp (exhaust)	Total Pressure (exhaust)	
	bars	lbf	lbm/sec	gpm	lbm/sec	Hz	deg F	inHg	psi
1	0.6	4.110	0	0	0.217	315	940	3.17	1.56
2	0.6	4.070	0.0023	0.0328	0.215	325.6	941	3.17	1.56
3	0.6	4.060	0.0024	0.0338	0.229	312.6		3.17	1.56
4			0.0027	0.0375	0.223	319		3.11	1.53
5			0.0025	0.0350	0.220	323		3.13	1.54
average		**4.08**	**0.0025**	**0.035**	**0.221**	**320.1**	**941**	**3.15**	**1.55**
9	0.8	5.806	0.0019	0.0265	0.255	420	975	4.70	2.31
10	0.8	5.806	0.0018	0.0250	0.268	443.5		4.70	2.31
11	0.8	5.805	0.0049	0.0695	0.256	434.8		4.68	2.30
12					0.252		977	4.66	2.29
average		**5.81**	**0.0029**	**0.040**	**0.258**	**432.8**	**976**	**4.68**	**2.30**
1	1.0	7.55	0.0000	0.000	0.294	494.4	1040	6.19	3.04
2	1.0	7.55	0.0031	0.043	0.282	492.6	1040	6.26	3.07
3	1.0	7.57	0.0041	0.057	0.276	491.2	1040	6.26	3.07
4	1.0	7.56	0.0035	0.050	0.288	488.7	1040	6.25	3.07
5	1.0	7.56	0.0035	0.049	0.286	494.6	1040	6.30	3.09
6	1.0	7.56	0.0039	0.055	0.287	501.3	1040	6.26	3.07
7	1.0	7.6	0.0036	0.051	0.284	493.6	1040	6.33	3.11
8	1.0	7.64	0.0038	0.054	0.269	508.3	1040	6.23	3.06
average		**7.57**	**0.0032**	**0.045**	**0.283**	**495.6**	**1040**	**6.26**	**3.07**

JPX run 30 MAY 1995								
			Fuel	Fuel	corrected		Exhaust	
Run	Pressure	Thrust	Flow	flow	Mass flow(air)	Temp	Pressure	
#	bars	lbf	lbm/sec	gpm	lbm/sec	deg F	inHg	psi
1	0.15	0.90	0.0000	0.000	0.100	933	0.69	0.34
2	0.15	0.86	0.0011	0.015	0.110		0.651	0.32
3	0.15	0.84	0.0012	0.017	0.097	931	0.6	0.29
4	0.15	0.82	0.0012	0.017	0.118		0.624	0.31
1	0.3	2.97	0.0000	0.000	0.174	882	1.62	0.80
2	0.3	2.50	0.0018	0.026	0.171		1.54	0.76
3	0.3	2.45	0.0018	0.025	0.174		1.54	0.76
4	0.3	2.46	0.0017	0.024	0.174		1.46	0.72
5	0.3	2.59	0.0018	0.025	0.172	883	1.61	0.79
6	0.4	1.85	0.0018	0.025	0.141		0.97	0.48
7	0.4	2.17	0.0016	0.022	0.132		0.97	0.48
8	0.4	1.65	0.0016	0.023	0.168	893	1.30	0.64
9	0.4	1.79	0.0017	0.023	0.128		1.12	0.55
10	0.4	1.73	0.0017	0.023	0.140	896	1.00	0.49
1	0.5	3.37	0	0.000	0.202	896	2.78	1.37
2	0.5	3.39	0.0020	0.028	0.179		2.66	1.31
3	0.5	3.36	0.0021	0.030	0.193		2.67	1.31
4	0.5	3.51	0.0024	0.034	0.196	894	2.81	1.38
5	0.5	3.51	0.0021	0.029	0.194		2.78	1.37
6	0.5	3.5	0.0021	0.030	0.185		2.68	1.32
7	0.5	3.43	0.0022	0.031	0.197		2.77	1.36
8	0.5	3.44	0.0022	0.031	0.191	895	2.75	1.35
1	0.7	5.12	0.0000	0.000	0.220		4.24	2.08
2	0.7	5.34	0.0028	0.039	0.245	974	4.37	2.15
3	0.7	5.49	0.0028	0.039	0.247		4.6	2.26
4	0.7	5.66	0.0030	0.043	0.236		4.68	2.30
5	0.7	5.63	0.0029	0.041	0.227		4.29	2.11
6	0.7	4.94	0.0029	0.040	0.221	962	4.01	1.97
7	0.7	4.94	0.0027	0.038	0.223		4.03	1.98
8	0.7	4.95	0.0028	0.040	0.216	957	4.01	1.97

Run #	Pressure bars	Thrust lbf	Fuel Flow lbm/sec	Fuel flow gpm	corrected Mass flow(air) lbm/sec	Temp deg F	Exhaust Pressure inHg	psi
1	0.8	5.79	0.0000	0.000	0.249		4.71	2.31
2	0.8	5.84	0.0029	0.041	0.247	960	4.7	2.31
3	0.8	5.84						
4	0.8	5.85	0.0030	0.042	0.249		4.75	2.33
5	0.8	5.85	0.0027	0.039	0.252		4.66	2.29
6	0.8	5.82	0.0032	0.044	0.261	976	4.7	2.31
7	0.8	5.83	0.0028	0.040	0.250		4.7	2.31
8	0.8	5.81	0.0029	0.041	0.243	977	4.73	2.32
1	0.9	6.58	0.0000	0.000	0.270		5.47	2.69
2	0.9	6.60	0.0033	0.046	0.273		5.36	2.63
3	0.9	6.53	0.0033	0.046	0.258	1009	5.37	2.64
4	0.9	6.57	0.0033	0.046	0.261		5.35	2.63
5	0.9	6.56	0.0033	0.047	0.268		5.27	2.59
6	0.9	6.55	0.0031	0.043	0.270	1003	5.32	2.61
7	0.9	6.55	0.0033	0.046	0.261		5.29	2.60
1	1.15	8.9	0.0000	0.000	0.297	1067	7.37	3.62
2	1.15	8.9	0.0039	0.056	0.301	1071	7.37	3.62
3	1.15	9.04	0.0039	0.056	0.298		7.39	3.63
4	1.15	9.11	0.0042	0.059	0.298		7.38	3.62
5	1.15	9.08	0.0041	0.058	0.302	1071	7.41	3.64
6	1.15	9.11	0.0041	0.058	0.303		7.43	3.65
7	1.15	9.12	0.0041	0.058	0.300		7.43	3.65
8	1.15	9.08	0.0041	0.058	0.302		7.37	3.62

					June 12 1995			
			Fuel	Fuel	corrected			Exhaust
Run	Pressure	Thrust	Flow	flow	Mass flow(air)	Temp		Pressure
#	bars	lbf	lbm/sec	gpm	lbm/sec	deg F	inHg	psi
1	1.15	9.12	0	0.000	0.305	1077	7.34	3.61
2	1.15	9.16	0.0039	0.056	0.303	1080	7.40	3.63
3	1.15	9.17	0.0041	0.057	0.307		7.38	3.63
4	1.15	9.14	0.0041	0.058	0.307	1079	7.42	3.65
5	1.15	9.34	0.0041	0.058	0.306		7.42	3.65
6	1.15	9.15	0.0041	0.058	0.303		7.18	3.53
	average	9.19	0.0041	0.057	0.305	1079.5	7.36	3.61
1	1.0	7.69			0.293	1035	6.26	3.07
2	1.0	7.76	0.0035	0.050	0.291	1038	6.30	3.09
3	1.0	7.83	0.0036	0.051	0.287		6.34	3.11
4	1.0	7.88	0.0036	0.051	0.287	1040	6.36	3.12
5	1.0	7.97	0.0040	0.056	0.293		6.43	3.16
6	1.0	7.99	0.0037	0.052	0.289		6.18	3.03
7	1.0	7.68	0.0037	0.052	0.275	1035	6.24	3.07
8	1.0	7.70	0.0034	0.048	0.286	1036	6.22	3.05
	average	7.81	0.0036	0.051	0.288	1037	6.29	3.09
1	0.8	5.92			0.246		4.77	2.34
2	0.8	5.93	0.0030	0.042	0.245	964	4.79	2.35
3	0.8	5.84	0.0029	0.041	0.249		4.65	2.28
4	0.8	5.81	0.0032	0.045	0.239		4.66	2.29
5	0.8	0.00	0.0000	0.000	0.253		4.66	2.29
6	0.8	5.81	0.0040	0.056	0.253		4.62	2.27
7	0.8	5.90	0.0028	0.040	0.251	971	4.74	2.33
8	0.8	5.85	0.0031	0.043	0.248	965	4.65	2.28
	average	5.87	0.0032	0.045	0.248	966.7	4.69	2.30
1	1.0	7.74			0.285	1028	6.239	3.06
2	1.0	7.56	0.0032	0.046	0.278	1029	6.147	3.02
3	1.0	7.63	0.0035	0.050	0.286		6.12	3.01
4	1.0	7.75	0.0036	0.050	0.284	1031	6.213	3.05
5	1.0	7.69	0.0036	0.051	0.285		6.12	3.01
6	1.0	7.65	0.0037	0.052	0.277	1030	6.187	3.04
7	1.0	7.70	0.0036	0.051	0.281	1030	6.239	3.06
8	1.0	7.63	0.0035	0.049	0.281	1031	6.147	3.02
	average	7.67	0.0035	0.050	0.282	1030	6.18	3.03

JUNE 12 1995								
					corrected	Total Temp	Total Pressure	
Run #	Pressure	Thrust	Fuel flow	Fuel flow	Mass flow (air)	(exhaust)	(exhaust)	
	bars	lbf	lbm/sec	gpm	lbm/sec	deg F	inHg	psi
1	0.15	0.90	0.0000	0.000	0.100	933	0.690	0.34
2	0.15	0.86	0.0011	0.015	0.110		0.651	0.32
3	0.15	0.84	0.0012	0.017	0.097	931	0.600	0.29
4	0.15	0.82	0.0012	0.017	0.118		0.624	0.31
	average	**0.85**	**0.0012**	**0.016**	**0.108**	**931**	**0.64**	**0.31**
6	0.3	1.85	0.0018	0.025	0.141		0.97	0.48
7	0.3	2.17	0.0016	0.022	0.132		0.97	0.48
8	0.3	1.65	0.0016	0.023	0.168	893	1.30	0.64
9	0.3	1.79	0.0017	0.023	0.128		1.12	0.55
10	0.3	1.73	0.0017	0.023	0.140	896	1.00	0.49
	average	**1.84**	**0.0017**	**0.023**	**0.142**	**895**	**1.07**	**0.53**
1	0.4	2.97	0.0000	0.000	0.174	882	1.62	0.80
2	0.4	2.50	0.0018	0.026	0.171		1.54	0.76
3	0.4	2.45	0.0018	0.025	0.174		1.54	0.76
4	0.4	2.46	0.0017	0.024	0.174		1.46	0.72
5	0.4	2.59	0.0018	0.025	0.172	883	1.61	0.79
	average	**2.59**	**0.0018**	**0.025**	**0.173**	**882.50**	**1.55**	**0.76**
1	0.5	3.37	0	0.000	0.202	896	2.78	1.37
2	0.5	3.39	0.0020	0.028	0.179		2.66	1.31
3	0.5	3.36	0.0021	0.030	0.193		2.67	1.31
4	0.5	3.51	0.0024	0.034	0.196	894	2.81	1.38
5	0.5	3.51	0.0021	0.029	0.194		2.78	1.37
6	0.5	3.5	0.0021	0.030	0.185		2.68	1.32
7	0.5	3.43	0.0022	0.031	0.197		2.77	1.36
8	0.5	3.44	0.0022	0.031	0.191	895	2.75	1.35
	average	**3.44**	**0.0022**	**0.031**	**0.192**	**895**	**2.74**	**1.34**
1	0.6	4.11	0.0000	0.000	0.217	940	3.17	1.56
2	0.6	4.07	0.0023	0.033	0.215	941	3.17	1.56
3	0.6	4.06	0.0024	0.034	0.229		3.17	1.56
	average	**4.08**	**0.0024**	**0.033**	**0.220**	**941**	**3.17**	**1.56**

1	0.7	5.12	0.0000	0.000	0.220		4.24	2.08
2	0.7	5.34	0.0028	0.039	0.245	974	4.37	2.15
3	0.7	5.49	0.0028	0.039	0.247		4.6	2.26
4	0.7	5.66	0.0030	0.043	0.236		4.68	2.30
5	0.7	5.63	0.0029	0.041	0.227		4.29	2.11
6	0.7	4.94	0.0029	0.040	0.221	962	4.01	1.97
7	0.7	4.94	0.0027	0.038	0.223		4.03	1.98
8	0.7	4.95	0.0028	0.040	0.216	957	4.01	1.97
	average	**5.26**	**0.0028**	**0.040**	**0.229**	**964**	**4.28**	**2.10**
1	0.8	5.79	0.0000	0.000	0.249		4.71	2.31
2	0.8	5.84	0.0029	0.041	0.247	960	4.7	2.31
3	0.8	5.84						
4	0.8	5.85	0.0030	0.042	0.249		4.75	2.33
5	0.8	5.85	0.0027	0.039	0.252		4.66	2.29
6	0.8	5.82	0.0032	0.044	0.261	959	4.70	2.31
7	0.8	5.83	0.0028	0.040	0.250		4.70	2.31
8	0.8	5.81	0.0029	0.041	0.243	960	4.73	2.32
	average	**5.83**	**0.0029**	**0.041**	**0.250**	**960**	**4.71**	**2.31**
1	0.9	6.58	0.0000	0.000	0.270		5.47	2.69
2	0.9	6.60	0.0033	0.046	0.273		5.36	2.63
3	0.9	6.53	0.0033	0.046	0.258	1009	5.37	2.64
4	0.9	6.57	0.0033	0.046	0.261		5.35	2.63
5	0.9	6.56	0.0033	0.047	0.268		5.27	2.59
6	0.9	6.55	0.0031	0.043	0.270	1003	5.32	2.61
7	0.9	6.55	0.0033	0.046	0.261		5.29	2.60
	average	**6.56**	**0.0032**	**0.046**	**0.266**	**1006**	**5.35**	**2.63**
1	1.0	7.55	0.0000	0.000	0.294	1040	6.19	3.04
2	1.0	7.55	0.0031	0.043	0.282	1040	6.26	3.07
3	1.0	7.57	0.0041	0.057	0.276	1040	6.26	3.07
4	1.0	7.56	0.0035	0.050	0.288	1040	6.25	3.07
5	1.0	7.56	0.0035	0.049	0.286	1040	6.30	3.09
6	1.0	7.56	0.0039	0.055	0.287	1040	6.26	3.07
7	1.0	7.6	0.0036	0.051	0.284	1040	6.33	3.11
8	1.0	7.64	0.0038	0.054	0.269	1040	6.23	3.06
	average	**7.57**	**0.0036**	**0.051**	**0.283**	**1040**	**6.26**	**3.07**

1	1.15	8.90	0.0000	0.000	0.297	1067	7.37	3.62
2	1.15	8.90	0.0039	0.056	0.301	1071	7.37	3.62
3	1.15	9.04	0.0039	0.056	0.298		7.39	3.63
4	1.15	9.11	0.0042	0.059	0.298		7.38	3.62
5	1.15	9.08	0.0041	0.058	0.302	1071	7.41	3.64
6	1.15	9.11	0.0041	0.058	0.303		7.43	3.65
7	1.15	9.12	0.0041	0.058	0.300		7.43	3.65
8	1.15	9.08	0.0041	0.058	0.302		7.37	3.62
	average	**9.04**	**0.0041**	**0.057**	**0.300**	**1070**	**7.39**	**3.63**

LIST OF REFERENCES

1. Department of Defense, Unmanned Aerial Vehicles 1994 Master Plan.

2. Aviation Week & Space Technology, *Turboprop Drone and Engine Under Study*, January 9, 1995.

3. Gill, P. W., Fundamentals of Internal Combustion Engines, United States Naval Institute, September, 1964.

4. "Jane's All the World's Aircraft, 1991-1992". Jane's Information Group.

5. Aviation Week & Space Technology, *Specifications*, March 16, 1992.

6. Dev, S. Paul, *Emerging Technologies for Gas Turbine Engines: UAV Synergies*, Paper AIAA 92-3757, Presented at AIAA/SAE/ASME/ASEE 28th Joint Propulsion Conference and Exhibit, July 1992, Nashville, TN.

7. Jennings, B. H. and Rogers, W L., Gas Turbine Analysis and Practice, McGraw-Hill Book Company, Inc. 1953.

8. NASA Conference Publication 2067, The Rotary Combustion Engine - a Candidate for General Aviation, Lewis Research Center Symposium, February 28, 1978.

9. Boyce, M.P., Gas Turbine Engineering Handbook, Gulf Publishing Company, 1982.

10. Mattingly, J., Heiser, W., and Daley, D., Aircraft Engine Design, New York, AIAA Education Series, 1987.

11. Mathur, A., "Estimation of Turbofan Engine Cycle Performance with and without a Wave Rotor Component", Naval Postgraduate School Contractor Report NPS67-86-006CR, Oct. 1986.

12. GASTURB User's Manual, A Program to Calculate Design and Off-Design Performance of Gas Turbines.

13. JPX TURBOREC T 240 Installation/Start Procedures/Technical Specification Manual.

14. A.S.M.E. Power Test Codes, Chapter 4, Flow Measurement - Instruments and Apparatus, PTC 19.5.

15. Wendland, R. A., Upgrade and Extension of the Data Acquisition System for Propulsion and Gas Dynamics Laboratories, M.S.A.E. Thesis, Naval Postgraduate School, Monterey, California, June 1992.

INITIAL DISTRIBUTION LIST

1.	Defense Technical InformationCenter Cameron Station Alexandria, Virginia 22304-6145	2
2.	Dudley Knox Library, Code 52 Naval Postgraduate School Monterey, California 93943-5101	2
3.	Director, Training and Education MCCDC, Code C46 1019 Elliot Rd. Quantico, Virginia 22134-5027	2
4.	Department of Aeronautics and Astronautics Naval Postgraduate School Monterey, California 93943-5002	
	ATTN: Chairman, Code AA	1
	ATTN: Professor R. P. Shreeve, Code AA/SF	10
	ATTN: Professor G. V. Hobson, Code AA/HG	1
5.	Commander Naval Air Systems Command Code AIR 4.4.T 1421 Jefferson Davis Highway Arlington, Virginia 22243	1
6.	Naval Air Warfare Center Aircraft Division Code AIR 4.4.3.1 [S. McAdams] Propulsion and Power Engineering, Bldg. 106 Patuxent River, Maryland 20670-5304	1
7.	Joint Projects and Demonstrations Directorate Attn: Ms. Malinda Pagett (UPR1) Washington, D.C. 20361-1014	1

8. S. Paul Dev 1
   D-STAR Engineering
   5-B Daisy Drive
   Seymour, Connecticut 06483

9. David P. Lobik 2
   School of Aviation Safety (AV) (Code 10)
   Naval Postgraduate School
   Monterey, California 93943-5002